

RESEARCH ARTICLE

# Dilution and titration of cell-cycle regulators may control cell size in budding yeast

Frank S. Heldt<sup>1\*</sup>, Reece Lunstone<sup>1</sup>, John J. Tyson<sup>2,3</sup>, Béla Novák<sup>1\*</sup>

**1** Department of Biochemistry, University of Oxford, Oxford, United Kingdom, **2** Department of Biological Sciences, Virginia Tech, Blacksburg, VA, United States of America, **3** Division of Systems Biology, Academy of Integrated Science, Virginia Tech, Blacksburg, VA, United States of America

\* stefan.heldt@bioch.ox.ac.uk (FSH); bela.novak@bioch.ox.ac.uk (BN)



## Abstract

The size of a cell sets the scale for all biochemical processes within it, thereby affecting cellular fitness and survival. Hence, cell size needs to be kept within certain limits and relatively constant over multiple generations. However, how cells measure their size and use this information to regulate growth and division remains controversial. Here, we present two mechanistic mathematical models of the budding yeast (*S. cerevisiae*) cell cycle to investigate competing hypotheses on size control: inhibitor dilution and titration of nuclear sites. Our results suggest that an inhibitor-dilution mechanism, in which cell growth dilutes the transcriptional inhibitor Whi5 against the constant activator Cln3, can facilitate size homeostasis. This is achieved by utilising a positive feedback loop to establish a fixed size threshold for the START transition, which efficiently couples cell growth to cell cycle progression. Yet, we show that inhibitor dilution cannot reproduce the size of mutants that alter the cell's overall ploidy and *WHI5* gene copy number. By contrast, size control through titration of Cln3 against a constant number of genomic binding sites for the transcription factor SBF recapitulates both size homeostasis and the size of these mutant strains. Moreover, this model produces an imperfect 'sizer' behaviour in G1 and a 'timer' in S/G2/M, which combine to yield an 'adder' over the whole cell cycle; an observation recently made in experiments. Hence, our model connects these phenomenological data with the molecular details of the cell cycle, providing a systems-level perspective of budding yeast size control.

## OPEN ACCESS

**Citation:** Heldt FS, Lunstone R, Tyson JJ, Novák B (2018) Dilution and titration of cell-cycle regulators may control cell size in budding yeast. PLoS Comput Biol 14(10): e1006548. <https://doi.org/10.1371/journal.pcbi.1006548>

**Editor:** Eric A. Sobie, Mount Sinai School of Medicine, UNITED STATES

**Received:** May 2, 2018

**Accepted:** October 5, 2018

**Published:** October 24, 2018

**Copyright:** © 2018 Heldt et al. This is an open access article distributed under the terms of the [Creative Commons Attribution License](https://creativecommons.org/licenses/by/4.0/), which permits unrestricted use, distribution, and reproduction in any medium, provided the original author and source are credited.

**Data Availability Statement:** All relevant data are within the paper and its Supporting Information files. The models are also available at [www.cellcycle.org.uk/publication](http://www.cellcycle.org.uk/publication) and were deposited in BioModels (MODEL1803220001 and MODEL1803220002).

**Funding:** FSH and BN are funded by the Biotechnology and Biological Sciences Research Council (BBSRC) Strategic LoLa grant BB/M00354X/1. JJT acknowledges financial support from the US National Institutes of Health (5R01-GM078989-12) administered through Colorado

## Author summary

Proliferating cells need to coordinate the initiation of genome replication and cell division with cell growth. In particular, the average time between two division events must precisely allow for a doubling in cell volume. Any systematic deviation from this balance would lead to progressive changes in cell size over consecutive generations and to a breakdown of biochemical processes. Here, we study two molecular mechanisms by which budding yeast cells might achieve this coordination. Through mathematical modelling, we show that the dilution of an inhibitor of cell cycle progression by cell growth can facilitate size homeostasis. But this mechanism fails to reproduce the size of mutant cells in which parts of the control machinery have been altered. By contrast, the titration of an activator

State University (PI: Jean Peccoud). The funders had no role in study design, data collection and analysis, decision to publish, or preparation of the manuscript.

**Competing interests:** The authors have declared that no competing interests exist.

against a constant number of genomic sites recapitulates these data and achieves size homeostasis. Since the control network of cell cycle progression in budding yeast is structurally similar to mammalian cells, our model could indicate a common mechanism for size control.

## Introduction

Balanced growth of proliferating cells requires some coordination between the increasing size of a growing cell and its probability of undergoing DNA synthesis and division. In particular, the average time between two successive cell divisions must allow for a doubling in cell mass (or volume, which we will use interchangeably in the following). Any systematic deviation from this balance would lead to progressive changes in size over consecutive generations, eventually leading to the breakdown of biochemical processes. However, despite mounting evidence for active size control in various cell types and across different organisms [1], if and how cells measure their size and relay this information to the cell cycle remains controversial [2].

An elegant way to coordinate cell division and growth is to restrict passage through a certain cell cycle stage to cells that are larger than a particular target size [1]. Such ‘size checkpoints’ have been proposed to underlie size control at the *START* transition in budding yeast [3–5], and at the *G2/M* transition in fission yeast [6–8] and slime mould plasmodia [9–11]. The critical size required to pass these transitions depends, among other things, on the ploidy of the cell and its nutritional status [2]. To establish a size checkpoint, cells need to generate a size-dependent biochemical signal. Yet, most cellular macromolecules increase in abundance proportionally to cell volume, so that their concentration remains constant and the reactions they are involved in are independent of size [12]. Several proteins that defy this general rule have been indicated in size control. The mitotic activator Cdc25, for instance, increases in concentration with size in fission yeast [8], while Whi5, an inhibitor of *START* in budding yeast, is diluted by cell growth [13]. This suggests a general mechanism, in which size control emerges from the interplay between size-dependent and size-independent cell cycle regulators. Here, we study this intriguing possibility, focusing on the budding yeast cell cycle.

The budding yeast *Saccharomyces cerevisiae* divides asymmetrically, with size control mainly operating in the new-born daughter cell when it commits to enter the cell cycle anew at the *START* transition [3–5]. Passage through *START* is driven by activation of the transcription factor SBF [14]. In early *G1*-phase, before *START*, SBF is kept inactive by its stoichiometric inhibitor Whi5 [15,16]. To enter the cell cycle, the cyclin-dependent kinase Cdk1 (encoded by the *CDC28* gene) in conjunction with its regulatory binding partner Cln3 phosphorylates Whi5, which partially liberates SBF from inhibition and induces the synthesis of other *G1* cyclins (Cln1 and Cln2). Cln1/2:Cdk1 complexes then accelerate the phosphorylation of Whi5 and activation of SBF, thereby promoting the *START* transition [15–17]. Recent experiments show that during *G1* the concentration of Cln3, the activator of *START*, is constant, while the concentration of Whi5 decreases, suggesting that an inhibitor-dilution mechanism facilitates size control [13]. However, previous theoretical considerations and experimental data suggested a different mechanism based on the titration of an activator that increases in molecule number during growth—as would be the case if its concentration is kept constant—against a fixed number of nuclear sites [18–20].

To test these hypotheses, we developed a mechanistic mathematical model of the budding yeast cell cycle. At its core, the model comprises a simple description of gene expression in which both size-dependent and size-independent synthesis of proteins emerge seamlessly

from the assumption of differential affinity of genes for ‘transcription machinery’. This allows size-dependent proteins to maintain a fixed concentration during growth without the need for complex, gene-specific regulation and for size-independent proteins to maintain a fixed number of molecules per cell. Together, such size-dependent and -independent proteins can generate size-dependent biochemical signals for progression through the cell cycle. Using this model, we show that an inhibitor-dilution mechanism can facilitate size homeostasis and correctly account for changes in protein synthesis observed in experiments that perturb the number of gene copies of cell cycle regulators as well as the overall ploidy of the cell. However, the model fails to reproduce changes in cell size seen in some of these mutants. Intriguingly, a combination of inhibitor dilution and the titration of an activator against genomic sites correctly recapitulates these changes in cell size. Such a model also produces cell size patterns consistent with a ‘sizer’ mechanism in G1 and a ‘timer’ period comprising S, G2 and M-phase, which combine to yield an ‘adder-type’ behaviour over the entire cell cycle; an observation recently made experimentally [21]. Hence, our model unites various experimental findings that were previously thought incompatible.

## Results

### A model for size-dependent and -independent protein expression

Experimental evidence suggests that size control emerges from the interplay of regulatory proteins whose synthesis rates depend on cell size and their size-independent counterparts [8,13]. To simulate the expression of such proteins we propose a simple mathematical model based on the differential binding of transcription machinery (TM) to genes (Fig 1A). We model cell growth by assuming that components of the TM are themselves synthesised from size-dependent genes, which makes the production of TM autocatalytic, and that products of size-dependent genes control the increase in cell volume. These simple assumptions result in an exponential rise in both the amount of TM and cell size over time (Fig 1B), as is characteristic for budding yeast both in single cells and at the population level [2,21].

We note that the accumulation of TM in our simulations is compatible with experimental data on RNA polymerase II, which has been implicated in global transcriptional control [22]. Moreover, cell growth in the model depends on proteins that are themselves made by TM, which naturally leads to a direct proportionality between cell volume and transcriptional capacity. More precisely, as cells produce more and more TM their volume growth rate increases by the same extent, such that the number of TM molecules per unit cell volume remains constant. The fact that larger cells contain more TM translates into an increased occupation of size-dependent genes by TM, while size-independent genes are already fully occupied in small cells due to their high affinity for TM (Fig 1C). Consequently, the transcriptional output from size-dependent genes increases with cell size, allowing their proteins to maintain a constant concentration during exponential cell growth (Fig 1D). By contrast, expression from size-independent genes remains almost constant, such that their proteins are diluted by cell growth. Note that protein transcription is a highly complex, non-equilibrium process involving the binding of transcription factors, chromatin remodelling and multiple layers of regulation [23,24], e.g. cell cycle and nutrient-dependent control. We propose that the basic size-related regulation shown here operates alongside these other mechanisms to compensate for changes in cell size. Furthermore, the two protein classes in Fig 1A represent extremes on either end of the binding-affinity spectrum. Intermediate expression patterns, including proteins that switch from being size-dependent to size-independent during cell growth, can arise in between these extremes (S1 Fig).

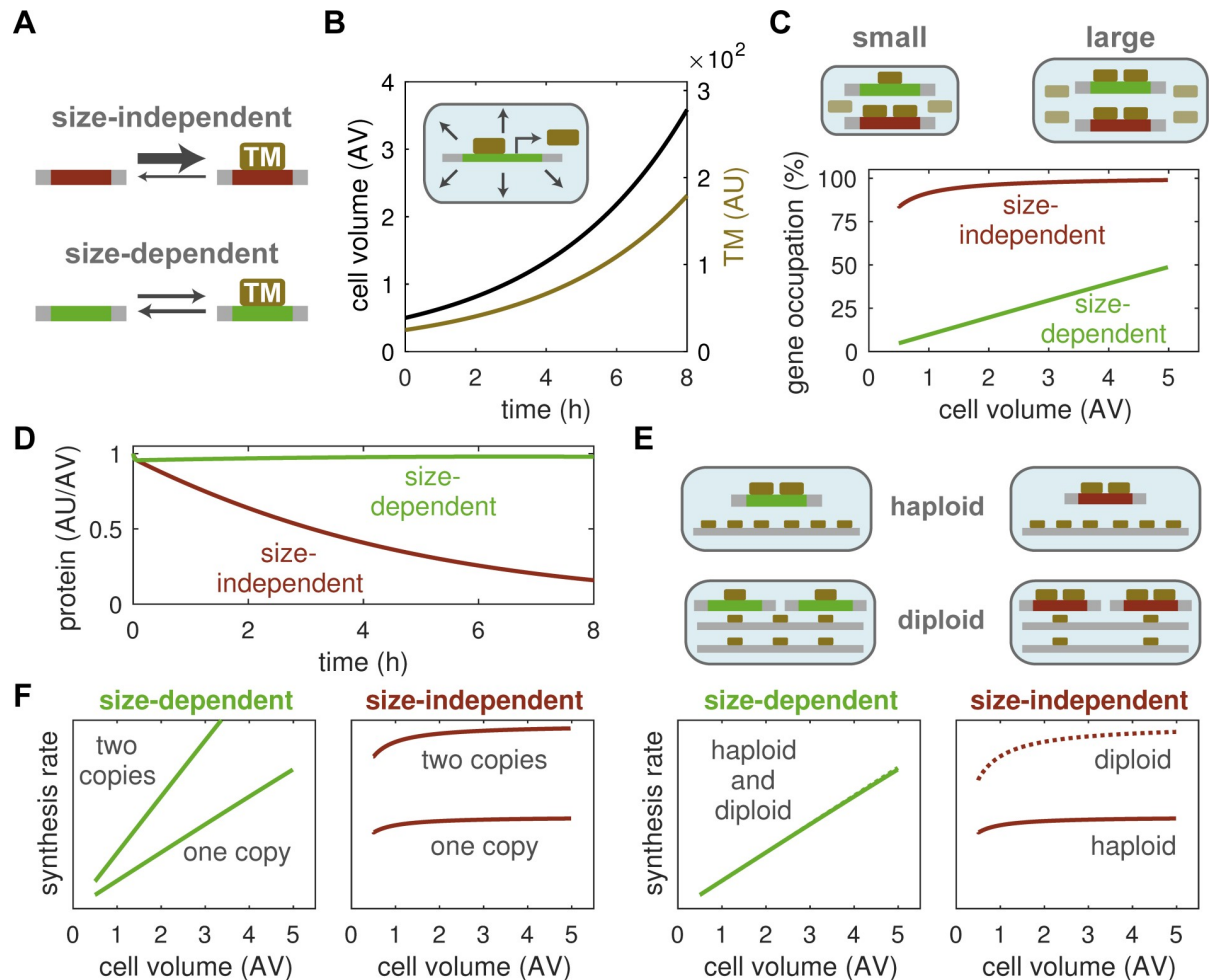


**Fig 1. A model for size-dependent and -independent gene expression.** (A) Transcription machinery (TM) binds with high affinity to the genes of size-independent proteins (top), while binding to the genes of size-dependent proteins is weaker (bottom). (B) Cell size and amount of TM in a model where growth and TM synthesis are controlled by size-dependent genes. (C) The amount of TM increases with cell size, which benefits the occupation of size-dependent genes, while size-independent genes are saturated early, at low levels of TM. (D) Concentration of a size-dependent and a size-independent protein in a growing cell. (E) An increase in ploidy does not affect the protein synthesis rate of size-dependent genes (left) as they share the available TM among each other and with the rest of the genome. Synthesis rates in haploid (solid) and diploid (dashed) cells overlap. Size-dependent genes (right) increase in expression in diploid cells as they sequester TM from the rest of the genome. (F) An additional gene copy in a haploid cell increases synthesis of both size-dependent (left) and size-independent (right) proteins. AU, arbitrary unit of number of molecules; AV, arbitrary unit of cell volume; AU/AV, arbitrary unit of concentration.

<https://doi.org/10.1371/journal.pcbi.1006548.g001>

Our gene expression model predicts that the two principal gene types react differently to a ploidy increase, i.e., a doubling of their copy number and of the rest of the genome. In particular, size-dependent genes compensate for ploidy by splitting TM between the two gene copies and the genome, whereas their size-independent counterparts compete efficiently for TM with other genes and increase in expression (Fig 1E). However, an additional gene copy in the absence of a ploidy increase leads to a higher expression of either gene type (Fig 1F). Hence, protein synthesis depends on the copy-number-to-ploidy ratio for size-dependent genes and strictly on the gene copy number for size-independent genes. In summary, our model uses a simple mechanism to explain why size-independent proteins are diluted by cell growth, whereas size-dependent proteins keep a constant concentration, without the need for complex, gene-specific regulation.

### Dilution of Whi5 can establish size control

Next, we asked whether the differential expression of cell cycle regulators according to the above model would allow budding yeast cells to control their size. In budding yeast, size control acts at *START* [3–5], where cells commit to cell cycle entry. Hence, we developed a cell cycle model centred on this transition (Fig 2A). In this model, passage through *START* is facilitated

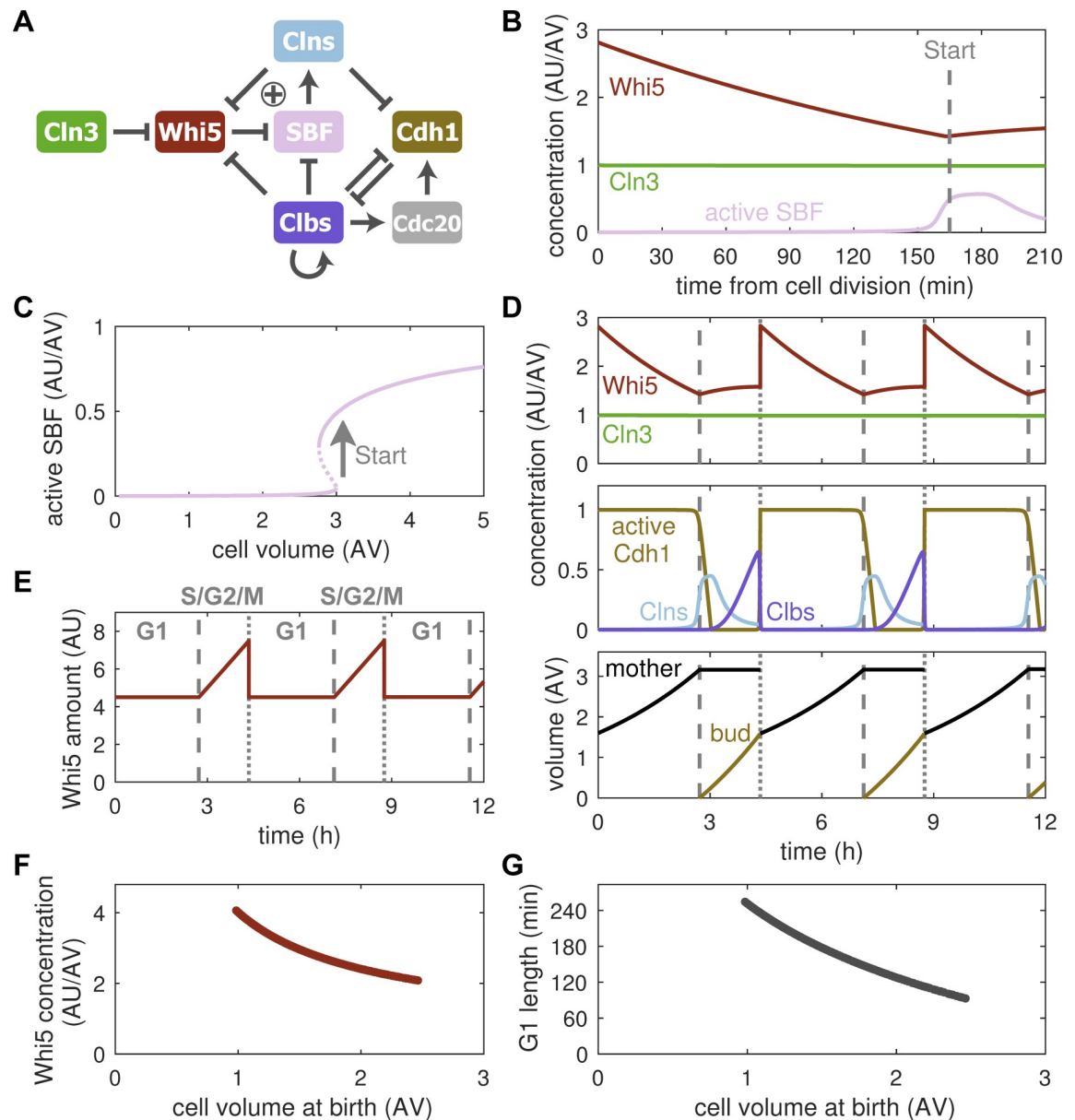


**Fig 2. Inhibitor dilution allows for size homeostasis.** (A) Influence diagram of the cell cycle model. Barbed edges indicate ‘activation’, blunt edges indicate ‘inhibition’, plus sign indicates positive feedback at *START*. The synthesis of all proteins except Whi5 is assumed to be size-dependent. (B) Concentration of the size-independent inhibitor of *START*, Whi5, and the size-dependent activator, Cln3, in G1-phase. Activation of SBF marks the onset of *START* (dashed line). (C) Stable (solid) and unstable (dashed) steady states of active SBF with respect to cell volume. Arrow indicates *START* transition. (D) Concentrations of cell cycle regulators (top and middle) and cell volume (bottom) over multiple generations. Dashed and dotted vertical lines mark *START* and cell division, respectively. Model follows the daughter cell (bud) after each division. (E) Simulated amount of Whi5 over multiple cell cycles. The G1-phase and S/G2/M period are indicated. (F) Correlation between Whi5 concentration and cell size at birth. Cell size was varied by changing the specific growth rate (see *Methods* for details). (G) Correlation between G1 length and cell size at birth.

<https://doi.org/10.1371/journal.pcbi.1006548.g002>

by the activation of SBF, which is opposed by the stoichiometric inhibitor Whi5. Through the phosphorylation of Whi5, Cln3 liberates SBF from inhibition, thus driving cell cycle entry (S2A Fig). Based on experimental observations [13], we assume that Whi5 is a size-independent gene, while all other proteins in our model are size-dependent. Consequently, cell growth in G1 dilutes the inhibitor of *START*, Whi5, while the activator Cln3 is maintained at constant concentration (Fig 2B), as has been observed experimentally [13]. Our model shows that this inhibitor-dilution mechanism can establish a size threshold for *START*, where SBF is relieved from Whi5 inhibition only after sufficient growth has occurred (Fig 2C). This transition is rapid and switch-like because of positive feedback via Cln1 and Cln2, which are expressed in response to SBF activation and further phosphorylate Whi5 [25,26]. The positive feedback loop creates a bistable switch, which implements the threshold response to graded changes in Whi5 concentration caused by cell volume growth, providing a sensitive size-sensing mechanism. After *START* has been passed, growth is restricted to the bud [4], and it continues until the end of the cycle, when the degradation of Clb1 and Clb2 initiates the separation of mother and daughter cell (Fig 2D). Intriguingly, our model readily shows size homeostasis over multiple generations (Fig 2D, lower panel). In particular, daughter cells, which we follow in our simulations because they show strong size control, reach the same size as their mothers, suggesting that Whi5 dilution can indeed couple cell division to cell growth.

In order to actively regulate cell size, i.e., to reduce size differences between cells, the inhibitor-dilution model requires that larger than average cells are born with lower than average Whi5 concentration so that they progress faster through G1, while smaller than average cells have higher Whi5 concentration, which gives them more time to grow. It has been proposed that this negative correlation between cell size at birth and Whi5 concentration results from the synthesis of a fixed amount of Whi5 during a period of fixed duration, which encompasses S-, G2- and M-phases in budding yeast [13]. By design our model accounts for this synthesis pattern, restricting Whi5 synthesis to the post-*START* period (Fig 2E). We find that new-born cells do indeed exhibit a size-dependent Whi5 concentration (Fig 2F). This allows for the adjustment of G1 duration to a cell's birth size (Fig 2G). In summary, our model demonstrates that size-independent synthesis of Whi5 and its dilution during G1 can allow cells to maintain their size over multiple generations by creating a cell-size threshold for *START*. Furthermore, the synthesis of a fixed amount of Whi5 per cell cycle can adjust for size differences by tuning G1 duration.

### Inhibitor-dilution model fails to reproduce all ploidy effects

To further explore the model's ability to reproduce size control, we compared it to experiments that vary the copy number of *CLN3* and *WHI5*, as well as the cell's overall ploidy [13]. These data were originally used to prove that Whi5's synthesis rate is independent of cell size, while Cln3's synthesis rate increases in larger cells ([13] and Fig 3A). These experiments also highlight that Whi5 synthesis is largely independent of ploidy, with only a slight decrease seen between haploid and diploid cells that harbour the same number of *WHI5* copies (Fig 3A, left panel). Yet, when the copy number of its gene is doubled, the Whi5 synthesis rate changes proportionally. Cln3 expression, in contrast, does change with ploidy, i.e., the slope of the synthesis rate decreases in diploid cells with one copy of *CLN3* compared to their haploid counterparts (Fig 3A, right panel). However, an increase in *CLN3* copy number does not affect the Cln3 synthesis rate as long as the ratio between copy number and ploidy is kept constant. Crucially, diploid cells (with two copies each of *WHI5* and *CLN3*) were shown to be roughly twice the size of haploid cells (with one copy each of *WHI5* and *CLN3*).

We simulated these copy-number mutants using the inhibitor-dilution model, which includes the features of gene expression shown in Fig 1. The resulting simulations correctly

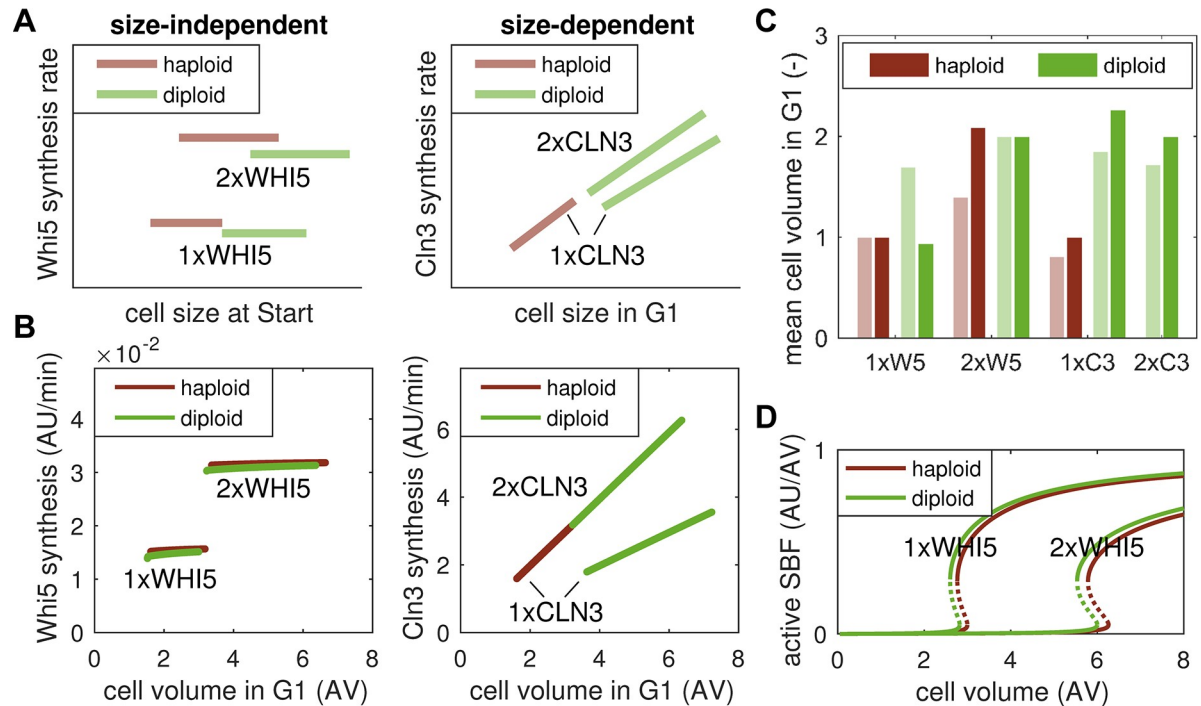


**Fig 3. Inhibitor-dilution model fails to capture all ploidy effects on size.** (A) Qualitative reproduction of experimental data in Fig 2F and G of Ref. [13]. Graphs show the synthesis rates of Whi5 and Cln3 in haploid and diploid cells with the indicated copy number of *WHI5* and *CLN3* genes. (B) Simulation of Whi5 and Cln3 synthesis rates in haploid and diploid cells with the indicated copy number of *WHI5* and *CLN3*. (C) Mean cell volume in G1 for data in A (light bars) and simulations in B (dark bars). Values were normalized to haploid cells with one *WHI5* copy for each case. (D) Stable (solid) and unstable (dashed) steady states of active SBF with respect to cell volume for haploid and diploid cells with one and two *WHI5* copies.

<https://doi.org/10.1371/journal.pcbi.1006548.g003>

predict the changes in protein synthesis rates for both Whi5 and Cln3 (Fig 3B). In particular, they recapitulate the copy-number dependence of Whi5 synthesis rate and the copy-number-to-ploidy dependence of Cln3 synthesis rate. The model also correctly predicts the two-fold size increase between haploid and diploid cells. However, our simulations fail to reproduce the size increase observed between haploid and diploid cells with the same number of *WHI5* copies (Fig 3C). More precisely, since protein synthesis rates for both Whi5 and Cln3 are similar in haploid and diploid cells with one *WHI5* copy (S3A Fig), the model predicts a similar size threshold for *START* (Fig 3D). In fact, considering the slight decrease in Whi5 synthesis rate observed in experiments [13], diploid cells with one *WHI5* should show a slight decrease in size compared to haploid cells according to our model. Reference [13] attributes the observed increase in cell size between haploid and diploid cells (with one or two copies of *WHI5*) to a delay in *S/G2/M* progression for diploid cells. Testing this hypothesis, we find that it only partially accounts for the observed size changes (S3B Fig). In particular, diploid cells with one *WHI5* are predicted to be smaller than haploid cells with two *WHI5*, suggesting a larger influence of Whi5 synthesis rate than ploidy (S3C Fig). However, in experiments the opposite is observed ([13] and Fig 3A). Moreover, a delay in *S/G2/M* progression together with the observed increase in Whi5 synthesis rate would lead to a more than two-fold difference between haploid and diploid cells (S3C Fig), in contradiction to experimental data [13]. Taken together, the inhibitor-dilution model thus correctly captures protein synthesis rates in copy-number and ploidy mutants but fails to reproduce the observed size increase for some diploid cells.

## Titration of nuclear sites can account for ploidy effect

Previous theoretical and experimental studies attributed the effects of ploidy on cell size to an alternative control mechanism relying on the titration of a protein with constant concentration against a fixed number of nuclear sites [9–11,18–20]. In particular, it has been suggested that Cln3 is titrated against SBF bindings sites on the genome [20]. Based on these suggestions, we augmented the inhibitor-dilution model with a titration mechanism to test whether these two concepts can be brought into unison (Fig 4A). In the pure inhibitor-dilution model, SBF, Whi5 and Cln3 interact in a strictly concentration-based manner (S2A Fig). By contrast, the titration model assumes that SBF occupies a fixed number of sites on the genome. In early G1 (i.e., in small daughter cells), these sites are filled with Whi5-inhibited SBF complexes to which Cln3 can bind tightly in a stoichiometric fashion. Once bound, Cln3 slowly hypo-phosphorylates Whi5 and dissociates in the process. However, it can rapidly rebound to unphosphorylated SBF:Whi5 (S2B Fig). As the cell grows larger, the number of Cln3 molecules per cell increases (Cln3 is a size-dependent protein, whose concentration is maintained constant in G1) (Fig 4B). This leads to a gradual accumulation of Cln3:Cdk1 heterodimers on Promoter:SBF:Whi5 complexes until all sites are filled, at which point free Cln3:Cdk1 kinase complexes emerge in the nucleus. Free Cln3:Cdk1 then promotes rapid hyper-phosphorylation of SBF-bound and free Whi5, facilitating the *START* transition (Fig 4B). Similar to the inhibitor-dilution model, the titration model readily yields size homeostasis in consecutive generations (Fig 4C) by coupling the passage through *START* to cell size (Fig 4D).

When simulating changes in gene copy number, we observe that, similar to inhibitor dilution, the titration model correctly predicts protein synthesis rates (Fig 4E). However, the titration mechanism also captures the increase in size between haploid and diploid cells with the same number of *WHI5* copies (Fig 4E). In particular, diploid cells harbour twice the number of SBF binding sites, which require a higher amount of Cln3, and therefore a larger cell size, to be filled (S4A Fig). Note that our model overestimates the size of diploid cells with one copy of *CLN3* (Fig 4F). The cause for this discrepancy is that the absence of a second *CLN3* copy in diploid cells only reduces Cln3 synthesis rate by ~15% (compare diploid cells with 1xCLN3 and 2xCLN3 in Fig 3A, right panel), whereas the model predicts a reduction by ~50% (Fig 4E, right panel). After accounting for this, cell size predictions are much more accurate (S4B and S4C Fig). It is not yet clear why a single *CLN3* can partially compensate for the second copy's expression rate in diploid cells.

Further experimental evidence for a titration mechanism comes from an observed increase in cell size upon transformation of otherwise wild-type cells with a high copy number plasmid containing perfect SBF binding sites [20]. These decoy sites were proposed to change the size threshold for *START* by binding Cln3 such that an increased number of Cln3 molecules, and hence a larger cell size, is required to initiate the transition. Simulating this setup, our model does indeed show such an increase in size (S4D Fig), providing further support for the existence a titration mechanism.

In summary, a combination of Whi5 dilution and Cln3 titration against SBF binding sites is not only able to capture protein synthesis rates but also the size of *WHI5*- and *CLN3*-mutant haploid and diploid cells and of cells harbouring an increased number of SBF binding sites.

## Sizer and timer combine to yield a phenomenological adder

Historically, three different strategies have been proposed to maintain cell size homeostasis: the sizer, where a cell cycle transition is triggered once the cells reaches a critical target size; the timer, whereby the cell cycle takes a constant amount of time; and the adder, postulating that cells add a constant volume each generation [27,28]. Each of these concepts may apply to the



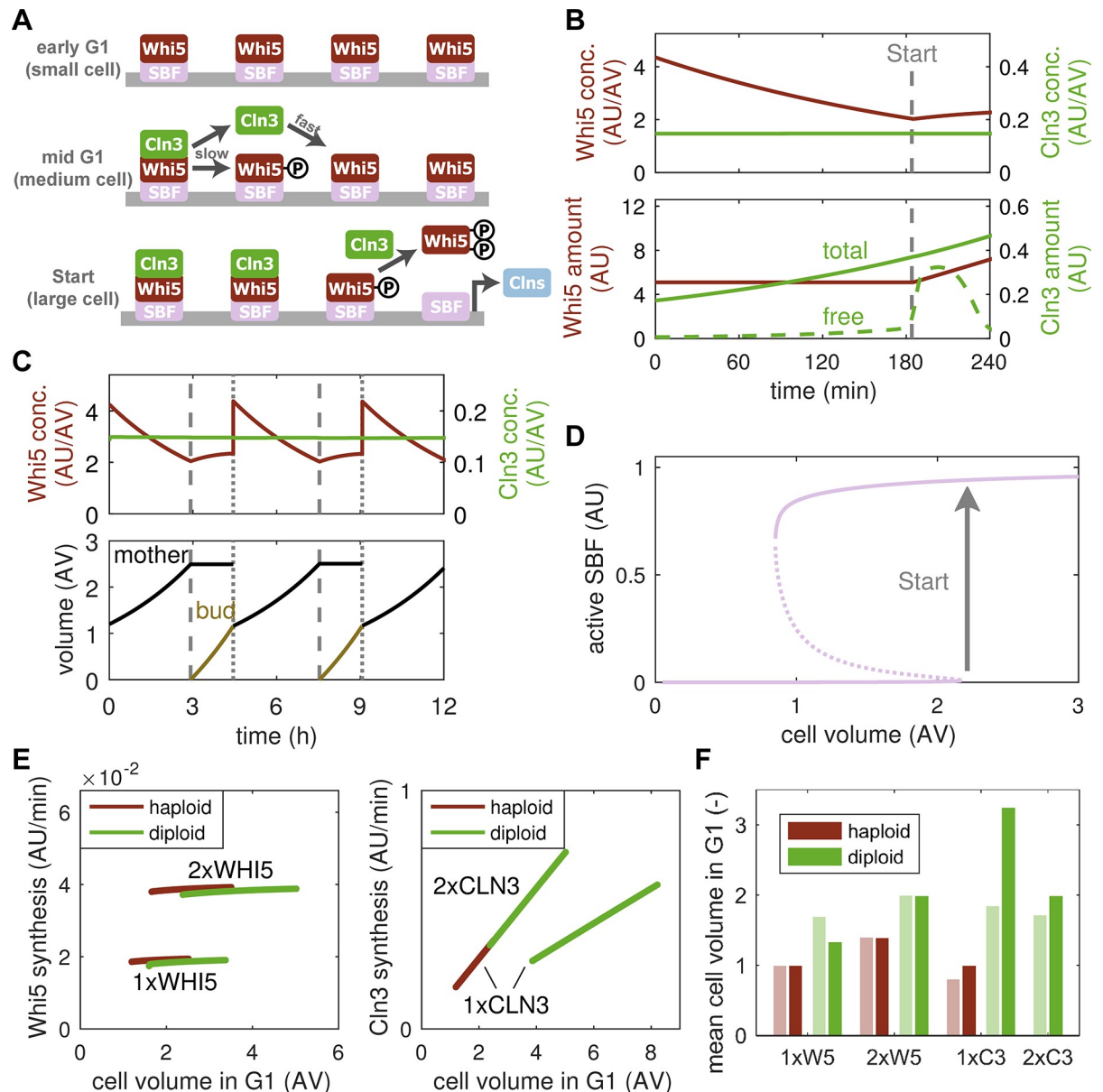


**Fig 4. Titration-of-nuclear-sites model captures ploidy effects on cell size.** (A) Schematic of the titration model. SBF occupies a fixed number of sites on the genome and is inhibited by Whi5 in early G1. Gradually accumulating Cln3:Cdk1 binds to and slowly hypo-phosphorylates Whi5. When all sites are filled (or hypo-phosphorylated), free Cln3 emerges and hyper-phosphorylates Whi5, liberating SBF. (B) Total concentration (top) and amount (bottom) of Whi5 and Cln3 in a growing cell. The amount of free Cln3 is indicated in the bottom panel (dashed green line). Vertical dashed line marks  $S_{TART}$ . (C) Concentration of cell cycle regulators (top) and cell volume (bottom) over multiple generations. Dashed and dotted vertical lines mark  $S_{TART}$  and division, respectively. Model follows the daughter cell (bud) after each division. (D) Stable (solid) and unstable (dashed) steady states of active SBF with respect to cell volume in the titration model. Arrow indicates  $S_{TART}$  transition. (E) Simulation of Whi5 and Cln3 synthesis rates in haploid and diploid cells with the indicated copy number of *WHI5* and *CLN3*. (F) Mean cell volume in G1 for data in [13] (light bars) and simulations in E (dark bars). Values were normalized to haploid cells with one *WHI5* copy for each case.

<https://doi.org/10.1371/journal.pcbi.1006548.g004>

complete cell cycle or only to a certain cell cycle phase, and all of them generate characteristic size patterns that can be probed experimentally (Fig 5A). An ideal sizer mechanism suggests that the final volume at the end of the sizer period is independent of the initial volume, such that the added volume shows a linear slope of minus one, i.e., small cells need to grow more to

reach the critical size. By contrast, exponentially growing cells that employ a perfect timer show a slope of plus one in the added volume as small cells grow less during the same time increment. Note that a slope of exactly one is only observed if cells double their mass within the phase that uses a timer, e.g. if the timer is employed over the whole cell cycle of a symmetrically dividing cell. Finally, an adder leads to a slope of zero since the added volume is assumed to be constant. We wanted to understand how these concepts connect to the mechanistic model of cell cycle control presented above.

Simulations of our titration model reveal that G1-phase behaves like an imperfect sizer with smaller cells adding more volume during G1 (slope of -0.64; Fig 5B, right panel) and cell size at S-phase entry showing a slight positive correlation with birth size (Fig 5B, left panel). S/G2/M-phases, by contrast, exhibit a timer (see also S5A Fig). The combination of a mechanistic sizer and a mechanistic timer yields a phenomenological adder with the added volume being virtually independent of cell size at birth ( $R = -0.02$ ; Fig 5B, right panel). However, the added volume is not directly sensed by the system in any way. Instead the negative slope of the sizer compensates for the positive slope of the timer.

The results above raise the question as to why cells employ two seemingly different strategies in G1 and S/G2/M-phases, a sizer and a timer, respectively. Presumably, S, G2 and M-phase are completed fast, with a size-independent timing, to allow the mother cell to start the next budding event, while size control is relegated to the daughter cell's G1 phase. In addition, a timer period of constant length in combination with a size-independent Whi5 synthesis allows the cell to produce a constant, size-independent amount of Whi5 per cell cycle (Figs 5C and 2E). This constant Whi5 amount is part of the mechanism that tunes G1 length with respect to birth size. Hence, the S/G2/M timer helps to set up the G1 sizer. We also note that our simulations show an imperfect sizer with a slight positive correlation between the cell volume at *START* and the birth volume (Fig 5B, left panel), as has been found experimentally [21,27]. Whereas an ideal sizer requires the size threshold for *START* to be independent of birth size, we find that cells which are larger at birth progress through *START* at a slightly larger size (Fig 5B and 5D). According to our model, the main reason for this threshold change is the distribution of Whi5 molecules at cell division. In particular, larger cells are born with slightly higher amounts of Whi5 (Fig 5E), since some of the Whi5-containing complexes are distributed according to the volume ratio of mother and daughter cell (Fig 5F). It is primarily by this mechanism that birth size affects the size threshold for *START* in our model, as shown in S5B Fig, where we manually set the Whi5 amount at birth to a constant value (birth size-independent) and find that the model behaves as an almost ideal G1 sizer.

In summary, our model shows that size control in budding yeast uses an S/G2/M timer that helps to produce a constant amount of Whi5 per cell cycle and to facilitate a sizer in the G1 phase of daughter cells. Both mechanism combine to yield a phenomenological adder over the whole cell cycle. However, the size-dependent distribution of Whi5 at cell division can cause an imperfect adjustment to size differences at birth.

## Discussion

Balanced growth, achieved by coupling cell division to the increase in cell mass, is crucial to cell survival as progressive changes in size over generations would eventually lead to a breakdown of biochemical processes. In this study, we developed a mechanistic mathematical model for size control in budding yeast based on the differential expression of cell cycle regulators in growing cells. We show that the interplay of size-dependent and size-independent synthesis of these regulators can establish a size threshold at *START* and facilitate size homeostasis.

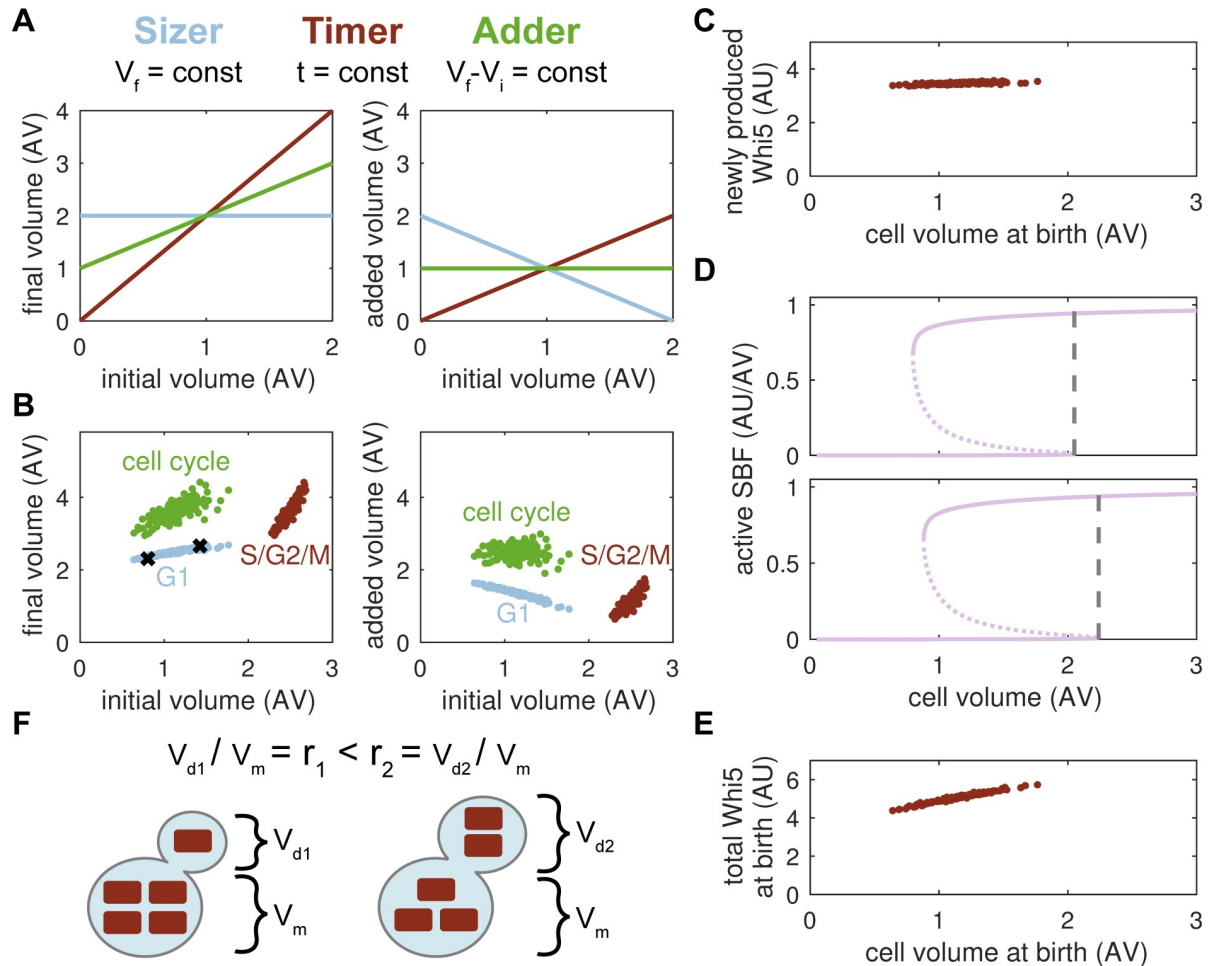


**Fig 5. G1 sizer and S/G2/M timer combine to yield adder.** (A) Theoretical predictions of the final volume ( $V_f$ ) and the added volume ( $V_f - V_i$ ) with respect to the initial volume ( $V_i$ ) for an ideal sizer, timer and adder. Simulations assume exponential growth and, for the timer, a doubling of cell mass. (B) Simulation of the final volume and added volume over the initial volume for G1-phase, S/G2/M-phases and the whole cell cycle in the titration model. Black crosses mark cells shown in D. (C) Amount of newly synthesised Whi5 in cells of different birth size. (D) Stable (solid) and unstable (dashed) steady states of active SBF with respect to cell volume for the two cells marked with black crosses in B. Dashed lines indicate size threshold for  $START$ . (E) Total amount of Whi5 at cell birth for cells of different birth size. (F) Scheme of Whi5 distribution at cell division. Whi5 that is not bound to the genome, i.e., which diffuses freely through the nucleus or cytoplasm (red rectangles), is distributed according to the volume ratio of mother and daughter cell ( $r$ ), which causes larger daughter cells to inherit more Whi5.  $V_d$ , daughter cell volume;  $V_m$ , mother cell volume.

<https://doi.org/10.1371/journal.pcbi.1006548.g005>

It has long been recognised that the amounts of most proteins in a cell increase with cell size [29,30], such that protein concentrations remain constant and reaction rates are unaffected by growth [12]. This has also been observed for the majority of cellular mRNAs, suggesting that adaptation to volume growth occurs at the transcriptional level [22,29,31–33]. Based on these observations, we propose a general mathematical model for gene expression in growing cells which assumes that a limiting component of the transcription machinery, which we named TM and that may correspond to an RNA polymerase or factors influencing chromatin accessibility [18], is produced in an autocatalytic manner by transcribing its own mRNA. Under conditions where nutrients and precursors are not limiting, this leads to an exponential increase in TM. If we assume that the increase in cell volume depends on proteins that are themselves transcribed by TM, the exponential rise in TM directly translates into an exponential increase in cell volume and it naturally leads to a direct proportionality between both, i.e.,

protein synthesis rates per unit volume remains constant. This scaling is an emergent property of the system and does not require complex regulation or a dedicated mechanism that measures size and tunes transcriptional capacity accordingly. In very large cells, genes become saturated, at which point transcription rates remain constant and cell growth transitions into a phase of linear increase. These features of the model are consistent with a large body of experimental literature showing exponential growth of cell volume and transcription for small cells which plateaus when cells exceed a certain size [12,21,22,27,34].

Given this model of gene expression, two different types of genes emerge in our simulations based on their affinity to TM. Genes that bind TM with high affinity are saturated early, in small cells, and thus show size-independent protein synthesis. Consequently, they give rise to size-independent proteins, whose amount is constant, leading to a decreasing concentration in growing cells. *Whi5* is an example of such a protein [13]. Due to their high affinity, size-independent genes compete efficiently for TM and an increase in their copy number, due to gene or genome duplication, directly translates into an increased synthesis and concentration. We hence propose that, in the context of size control, size-independent genes can act as gene-copy-number sensors. Beyond size regulation, the genes might encode proteins that need to be present in a fixed proportion to the genome content, e.g., transcription factors or histones. By contrast, size-dependent genes bind TM with lower affinity, such that their occupation by TM increases proportional to cell volume. Through this mechanism, their proteins can maintain a constant concentration until the gene is saturated. We propose that the majority of proteins uses this type of control, *Cln3* being a concrete example [13]. Due to their characteristics, size-dependent genes share TM among themselves, such that an overall ploidy increase does not result in an increase in protein concentration. Size-dependent genes can hence act as sensors for the copy-number-to-ploidy ratio, the gene dosage. Variations of the affinity constants between the two extremes may lead to intermediate expression patterns, including genes that can switch from size-dependent to size-independent expression within a given range of cell sizes. We propose that this simple mechanism of gene expression operates alongside other forms of transcription control, which involves non-equilibrium processes and stochastic phenomena [23,24], to compensate for cell growth.

By incorporating the gene expression model into a model of the yeast cell cycle, we show that size-independent synthesis of the inhibitor *Whi5* and size-dependent synthesis of the activator *Cln3*, a mechanism termed inhibitor dilution [13], can indeed establish size control at *START*. It is important to note that, because *Whi5* is a stoichiometric inhibitor of SBF without catalytic activity [15,16], we have assumed in our inhibitor-dilution mechanism that *Whi5* and SBF form a tightly bound complex. In addition, we assumed that phosphorylation of *Whi5* by *Cln3* breaks up the complex and liberates SBF. Considering that SBF maintains a constant concentration, as has been shown experimentally for one of its subunits [13], *Whi5* is therefore in fact countered by two size-dependent activators, *Cln3* and SBF. Given these molecular interactions, our results suggest that, in the inhibitor-dilution paradigm, the rising number of SBF molecules in a growing cell eventually overcomes inhibition by exceeding the constant number of *Whi5* molecules (see *S1 Text* for details). *Cln3* merely sets the threshold at which SBF activation occurs by keeping a fraction of *Whi5* molecules in a phosphorylated (inactive) state. Because this fraction does not change appreciably with cell size, *Cln3* is not directly involved in creating the size-dependent signal that facilitates *START* in our version of the inhibitor-dilution model. Hence, between the inhibitor-dilution model and the titration-of-nuclear-sites mechanism there exists an intriguing symmetry, in which *Whi5* and nuclear sites are very much alike. Both are constant in number and proportional to DNA content and both titrate away an activator. We also show that the gradual increase in SBF activity in response to cell volume growth that is caused by *Whi5* dilution is converted into an all-or-nothing decision by

a bistable switch located at *START*. This switch is created by a positive feedback loop on SBF activity and it establishes a strict size threshold of *START*. Hence, positive feedback and bistability are used to implement a size checkpoint in G1.

While inhibitor dilution is able to maintain size homeostasis and reproduce the size increase seen in diploid cells, it fails to explain why an increase in ploidy at a constant number of *WHI5* copies leads to larger cells. Such a change does not alter the expression of *Whi5* and *Cln3* and hence should not affect cell size at *START*. Even the delay in S/G2/M progression observed experimentally [13] is unable to reproduce these size changes in our model, suggesting that ploidy influences cell size beyond an effect through *Whi5* and *Cln3* expression and S/G2/M duration. Such an effect could be mediated by an as-yet-unknown inhibitor of *START* which is produced in a size-independent manner similar to *Whi5*. In this case, an increased expression of this inhibitor in diploid cells, due to a higher copy number of its gene, would cause the observed size increase. However, a much more appealing hypothesis is that the genome itself acts as an inhibitor of *START*. In particular, the binding of SBF to a limited number of genomic sites, which was proposed based on experiments [20], essentially converts SBF into a variable that does not change in number with cell size, as only the SBF that is bound to the genome would affect the *START* transition. Since the number of *Whi5* molecules is constant as well, the amount of *Whi5*:SBF complexes, assuming tight binding between both, is not changing with cell size. However, the number of *Cln3* molecules increases, such that *Cln3* titrates against *Whi5*:SBF complexes on the genome. At a particular threshold size, *Cln3* exceeds the number of *Whi5*:SBF complexes, leading to a sharp increase in free *Cln3* that can trigger *START*. Positive feedback is again used to convert this increase into an all-or-none decision. In this context, a diploid cell is larger because it contains twice the number of SBF binding sites, requiring more *Cln3* molecules to trigger *START*. Hence, the genome itself, through providing SBF binding sites that titrate *Cln3*, acts as a *START* inhibitor, using a form of distributed control (binding sites distributed throughout the genome) instead of a single gene product such as *Whi5*. We show that this *Cln3* titration model is consistent with *WHI5* and *CLN3* mutant phenotypes and with experiments in which additional SBF binding sites are expressed and consequently cell size at *START* is increased [20]. Also note that size-independent synthesis of *Whi5* in the titration model is beneficial because increasing *Whi5* production in large cells would impair their progress through *START*, thereby compromising size control. Moreover, the proportional increase in *Whi5* synthesis with gene copy number allows for a constant ratio between *Whi5* and SBF molecules on binding sites in cells with increasing ploidy, providing an intriguing hypothesis for why *Whi5* is synthesised in a size-independent manner.

A recent study of cell cycle commitment in budding yeast called into question the dilution of *Whi5*, arguing instead that a size-dependent increase in the concentrations of G1/S transcription factors helps to set the size threshold for *START* [35]. In S6 Fig, we show that such a model is indeed able to achieve size homeostasis but is incompatible with data on *Whi5* synthesis rates and the size of some mutant strains (see S2 Text for details). Hence, our model in combination with careful measurements of not only protein concentrations but also protein synthesis rates and cell sizes in mutants could help to resolve such discrepancies.

In recent years, studies of bacterial size control have argued for an ‘adder-type’ mechanism, whereby cells add a constant increment of cell mass per cycle [36,37]. A similar type of behaviour was found between two budding events in *S. cerevisiae* [34]. Yet, it remained unclear whether cells actively sense the added mass and use this information to regulate cell cycle events, a scenario later referred to as a mechanistic adder [21]. From our simulations, we indeed observe the presence of an adder over the whole cell cycle, with no correlation between the added cell mass and the volume at birth. However, this behaviour does not result from a direct mechanism, but rather from a combination of a mechanistic sizer in G1 and a mechanistic

timer in S/G2/M, which is in excellent agreement with a recent study arguing that the adder phenomenon emerges from independent pre- and post-START controls [21]. Similar to these and other experiments [5,21], our titration model shows an inverse proportionality between G1 length and birth size, and an imperfect sizer mechanism. We propose that adaptation is imperfect because of a volume-dependent distribution of Whi5. An ideal sizer, where START size is independent of birth size, requires that each daughter cell receives a constant amount of Whi5. However, Whi5 complexes that diffuse freely in the nucleus or cytoplasm would be distributed based on the size of the daughter cell, with large cells receiving a larger increment of Whi5 that keeps them in G1 for longer. In our model, this results in a weak birth-size dependence of the START threshold and imperfect size control. This might be one reason why cells do not rely on a pure inhibitor-dilution mechanism, which would exacerbate the influence of Whi5 distribution, but instead use a combination of Whi5 dilution and Cln3 titration. In addition, Cln3 is a highly unstable protein [38], and thus provides a snapshot of the current transcriptional capacity and volume of a cell, while Whi5 was produced in the previous cycle, inevitably introducing some form of memory of past growth conditions.

In summary, our study provides a mechanistic model of gene expression and cell cycle regulation in budding yeast that readily shows size homeostasis. Since the control network of START in budding yeast is structurally similar to restriction point control in mammalian cells, similar mechanisms could be at work during mammalian size control.

## Methods

### Mathematical modelling

Our models for budding yeast size control comprise sets of ordinary differential equations (ODEs). These ODEs describe the dynamics of genes and proteins in terms of their molecule number rather than concentration, which is used by most biochemical models that do not account for cell volume growth. In the following, we explain each of the two models (inhibitor dilution and titration of nuclear sites) in detail, starting with a generic description of gene expression that underlies both models.

**Gene expression.** Gene expression was modelled with the aim to capture the size-dependent and size-independent synthesis of proteins, which causes them to maintain their concentration or become diluted by cell growth, respectively. As these two types of regulation occur at the transcriptional level [12,22], we accounted for the amount of transcription machinery (*TM*). In our model, TM can bind to size-independent (*GI*) and size-dependent (*GD*) genes, leading to the formation of TM-gene complexes (*GITM* and *GDTM*, respectively).

$$\frac{d(TM)}{dt} = r_{TM}^{Sy} + k_{GITM}^{Ds} \cdot GITM + k_{GDTM}^{Ds} \cdot GDTM - \left( \frac{k_{GITM}^{As}}{V_t} GI + \frac{k_{GDTM}^{As}}{V_t} GD \right) \cdot TM, \quad (1)$$

$$\frac{d(GITM)}{dt} = \frac{k_{GITM}^{As}}{V_t} \cdot GI \cdot TM - k_{GITM}^{Ds} \cdot GITM, \quad (2)$$

$$\frac{d(GDTM)}{dt} = \frac{k_{GDTM}^{As}}{V_t} \cdot GD \cdot TM - k_{GDTM}^{Ds} \cdot GDTM, \quad (3)$$

where association rates are denoted  $k_{GITM}^{As}$  and  $k_{GDTM}^{As}$ , and dissociation rates are  $k_{GITM}^{Ds}$  and  $k_{GDTM}^{Ds}$ . The main difference between both gene types is their binding affinity, i.e., size-independent genes bind more tightly to TM ( $k_{GITM}^{As}/k_{GITM}^{Ds} > k_{GDTM}^{As}/k_{GDTM}^{Ds}$ ). Furthermore, we assumed that TM is stable and synthesised with rate  $r_{TM}^{Sy}$  (see Eq 5). Note that the rate of a bimolecular

(binding) reaction is inversely proportional to the total volume ( $V_t$ ) of the system, reflecting the fact that two molecules have a harder time finding each other inside a larger volume [39]. This volume may increase according to

$$\frac{d(V_t)}{dt} = r_{V_o}^{Sy}, \tag{4}$$

with the volume synthesis rate  $r_{V_o}^{Sy}$  (see Eq 6). Since the amount of most proteins in a cell increases with cell size [12,29,30], i.e., their synthesis is size-dependent, and proteins themselves are directly or indirectly responsible for cell volume growth, we assumed that both the synthesis rate of TM and cell volume are proportional to the number of transcriptionally active size-dependent genes ( $GDTM$ ).

$$r_{Tm}^{Sy} = k_{Tm}^{Sy} \cdot GDTM \cdot \frac{GCN}{GD_t}, \tag{5}$$

$$r_{V_o}^{Sy} = k_{V_o}^{Sy} \cdot GDTM \cdot \frac{GCN}{GD_t}. \tag{6}$$

Here,  $k_{Tm}^{Sy}$  and  $k_{V_o}^{Sy}$  are the rate constants for TM and volume synthesis, respectively. Note that in a haploid cell only one of all size-dependent genes ( $GD_t$ ) would be expected to encode for a specific protein, which is why we scale the synthesis rates using the gene copy number ( $GCN$ ). Following this scheme, size-independent ( $P_i$ ) and size-dependent ( $P_d$ ) proteins accumulate according to

$$\frac{d(P_i)}{dt} = k_{P_i}^{Sy} \cdot GITM \cdot \frac{GCN}{GI_t} - k_{P_i}^{De} P_i, \tag{7}$$

$$\frac{d(P_d)}{dt} = k_{P_d}^{Sy} \cdot GDTM \cdot \frac{GCN}{GD_t} - k_{P_d}^{De} P_d, \tag{8}$$

with  $GI_t = GI + GITM$  and  $GD_t = GD + GDTM$ ,

where  $k_{P_i}^{Sy}$  and  $k_{P_d}^{Sy}$  are rate constants for protein synthesis, and protein degradation rates are denoted  $k_{P_i}^{De}$  and  $k_{P_d}^{De}$ . Conservation equations hold for the total number of size-independent and size-dependent genes ( $GI_t$  and  $GD_t$ , respectively). This generic model for gene expression is used in the following to describe budding yeast size control in both the inhibitor-dilution and nuclear-sites-titration models.

**Inhibitor-dilution model.** Using the principles of gene expression described above (Eqs 1–6), we developed a model of the yeast cell cycle that accounts for cell volume growth and size control through inhibitor dilution. In particular, the volume of the mother cell ( $V_m$ ) and the daughter cell ( $V_d$ ), i.e., the bud, grow according to

$$\frac{d(V_m)}{dt} = Gr_m \cdot k_{V_o}^{Sy} \cdot GDTM \cdot \frac{GCN}{GD_t}, \tag{9}$$

$$\frac{d(V_d)}{dt} = Gr_d \cdot k_{V_o}^{Sy} \cdot GDTM \cdot \frac{GCN}{GD_t}, \tag{10}$$

with  $V_t = V_m + V_d$ ,

where  $Gr_m$  and  $Gr_d$  are binary variables that control whether growth is directed into the mother or daughter. These variables were introduced based on experimental observations

suggesting that, during the budded period, volume growth primarily occurs in the bud and not the parent cell [4]. Note that during the budded period, the total cell volume ( $V_t$ ) comprises the volume of both mother and daughter.

In our model, cell cycle progression occurs through the expression of three types of cyclins: the G1 cyclins Cln3 ( $CLN3$ ) and Cln1/2 ( $CLN$ ), and the mitotic cyclins Clb1/2 ( $CLB$ ).

$$\frac{d(CLN3)}{dt} = r_{Cln3}^{Sy} - k_{Cln3}^{De} \cdot CLN3, \quad (11)$$

$$\frac{d(CLN)}{dt} = r_{Cln}^{Sy} - k_{Cln}^{De} \cdot CLN, \quad (12)$$

$$\frac{d(CLB)}{dt} = r_{Clb}^{Sy} - r_{Clb}^{De} \cdot CLB, \quad (13)$$

with  $r_{Cln3}^{Sy}$ ,  $r_{Cln}^{Sy}$  and  $r_{Clb}^{Sy}$  denoting synthesis rates, and  $k_{Cln3}^{De}$ ,  $k_{Cln}^{De}$  and  $r_{Clb}^{De}$  degradation rates. These rates were defined as follows:

$$r_{Cln3}^{Sy} = k_{Cln3}^{Sy} \cdot GDTM \cdot \frac{GC_t}{GD_t}, \quad (14)$$

$$r_{Cln}^{Sy} = k_{Cln}^{Sy} \cdot GDTM \cdot \frac{GCN}{GD_t} \cdot \frac{SBF}{SBF_t} \cdot \frac{SBF_u}{SBF_t}, \quad (15)$$

$$r_{Clb}^{Sy} = \left( k_{Clb}^{Sy} + \frac{k_{ClbClb}^{Sy} \cdot CLB/V_t}{j_{Clb}^{Sy} + CLB/V_t} \right) \cdot GDTM \cdot \frac{GCN}{GD_t}, \quad (16)$$

$$r_{Clb}^{De} = k_{Clb}^{De} + \frac{k_{ClbCdh}^{De}}{V_t} \cdot CDH_a, \quad (17)$$

where  $k_{Cln3}^{Sy}$ ,  $k_{Cln}^{Sy}$  and  $k_{Clb}^{Sy}$  are the rate constants for constitutive synthesis, and  $k_{Clb}^{De}$  the rate constant for constitutive Clb1/2 degradation. All three proteins were assumed to be size-dependent, as are the majority of cellular proteins [12,29,30]. Note that we introduced a parameter for the copy number of the  $CLN3$  gene ( $GC_t$ ) to vary it independently from overall cell ploidy ( $GCN$ ). Since expression of Cln1/2 depends on the SBF transcription factor [40], we scaled the Cln synthesis rate by the fraction of free (not inhibited by Whi5; see Eq 20) SBF ( $SBF$ ) to total SBF ( $SBF_t$ ). Furthermore, SBF can become inhibited through phosphorylation by B-type cyclins in the later stages of the cell cycle [41]. Hence, Cln1/2 synthesis is also scaled by the fraction of unphosphorylated SBF ( $SBF_u$ ; Eq 22). For Clb1/2, we assumed that, in addition to constitutive production ( $k_{Clb}^{Sy}$ ), there is auto-activation [41] with maximal rate  $k_{ClbClb}^{Sy}$  and a Michaelis-type constant  $j_{Clb}^{Sy}$ , which causes saturation of the rate at high Clb1/2 levels. Note that auto-activation in this equation depends on the concentration of Clb1/2; hence, we divided by the total cell volume ( $V_t$ ). Finally, the degradation of Clb1/2 depends on a constitutive rate ( $k_{Clb}^{De}$ ) and on degradation by active APC/C<sup>Cdh1</sup> ( $CDH_a$ ) with rate constant  $k_{ClbCdh}^{De}$  in a concentration-dependent manner [42].

In the inhibitor-dilution model, Whi5 ( $WHI$ ) and free SBF ( $SBF$ ) bind in a concentration-based manner to form Whi5:SBF complexes ( $WHISBF$ ) that are devoid of activity, while



phosphorylated *Whi5* ( $WHI_p$ ) is unable to inhibit SBF [15,16].

$$\frac{d(WHI)}{dt} = -r_{Whi}^{Ph} \cdot WHI + k_{Whi}^{Dp} \cdot WHI_p - \frac{k_{WhiSbf}^{As}}{V_t} \cdot SBF \cdot WHI + k_{WhiSbf}^{Ds} \cdot WHISBF, \quad (18)$$

$$\frac{d(WHI_p)}{dt} = r_{Whi}^{Ph} \cdot WHI - k_{Whi}^{Dp} \cdot WHI_p + r_{Whi}^{Ph} \cdot WHISBF, \quad (19)$$

$$\frac{d(SBF)}{dt} = r_{Sbf}^{Sy} + r_{Whi}^{Ph} \cdot WHISBF - \frac{k_{WhiSbf}^{As}}{V_t} \cdot SBF \cdot WHI + k_{WhiSbf}^{Ds} \cdot WHISBF, \quad (20)$$

$$\frac{d(WHISBF)}{dt} = -r_{Whi}^{Ph} \cdot WHISBF + \frac{k_{WhiSbf}^{As}}{V_t} \cdot SBF \cdot WHI - k_{WhiSbf}^{Ds} \cdot WHISBF, \quad (21)$$

where association and dissociation rates for *Whi5* and SBF are denoted  $k_{WhiSbf}^{As}$  and  $k_{WhiSbf}^{Ds}$ , respectively. The phosphorylation and dephosphorylation rates of *Whi5* are  $r_{Whi}^{Ph}$  (see Eq 26) and  $k_{Whi}^{Dp}$ , respectively. Note that the phosphorylation of *Whi5* in *Whi5:SBF* complexes leads to their dissociation, which activates SBF. SBF is synthesised with rate  $r_{Sbf}^{Sy}$  (see Eq 25).

We assumed that the inhibitory phosphorylation of SBF is independent of its binding status and hence treated the state variables of phosphorylated ( $SBF_p$ ) and unphosphorylated ( $SBF_u$ ) SBF independent from the SBF variables shown above.

$$\frac{d(SBF_p)}{dt} = r_{Sbf}^{Ph} \cdot SBF_u - k_{Sbf}^{Dp} \cdot SBF_p, \quad (22)$$

$$\text{with } SBF_u = SBF_t - SBF_p \text{ and } SBF_t = SBF + WHISBF.$$

Here,  $r_{Sbf}^{Ph}$  (see Eq 27) and  $k_{Sbf}^{Dp}$  represent inhibitory phosphorylation and dephosphorylation of SBF, respectively. Conservation equations hold for the total amount of SBF ( $SBF_t$ ).

Production of *Whi5* is restricted to *S/G2/M* phases, i.e., the budded period, and daughter cells receive a larger proportion of *Whi5* at cell division [13]. Hence, we introduced newly produced *Whi5* ( $WHI_n$ ) and tied its synthesis to the binary variable for bud growth ( $Gr_d$ ).

$$\frac{d(WHI_n)}{dt} = r_{Whi}^{Sy} \cdot Gr_d, \quad (23)$$

where the rate of *Whi5* synthesis is denoted  $r_{Whi}^{Sy}$  (see Eq 24).

The synthesis and phosphorylation rates for the equations above were defined as follows:

$$r_{Whi}^{Sy} = k_{Whi}^{Sy} \cdot GITM \cdot \frac{GW_t}{GI_t}, \quad (24)$$

$$r_{Sbf}^{Sy} = k_{Vo}^{Sy} \cdot GDTM \cdot \frac{GCN}{GD_t}, \quad (25)$$

$$r_{Whi}^{Ph} = (k_{WhiCln3}^{Ph} \cdot CLN3 + k_{WhiCln}^{Ph} \cdot CLN + k_{WhiClb}^{Ph} \cdot CLB) / V_t, \quad (26)$$

$$r_{Sbf}^{Ph} = k_{SbfClb}^{Ph} \cdot CLB / V_t. \quad (27)$$

Here, *Whi5* synthesis occurs with rate constant  $k_{Whi}^{Sy}$  from a size-independent gene [13] with copy number  $GW_t$ , which we introduced to vary the number of *WHI5* copies independently of ploidy. *Whi5* is the only size-independent protein in the model ( $GI_t = GW_t$ ). Without loss of

generality, SBF synthesis was assumed to occur with the same rate as cell volume synthesis ( $k_{V_o}^{Sy}$ ), such that the SBF concentration remains constant at 1 AU/AV. In our model, Whi5 is phosphorylated by Cln3, Cln1/2 and Clb1/2 [15–17] with rates  $k_{WhiCln3}^{Ph}$ ,  $k_{WhiCln}^{Ph}$  and  $k_{WhiClb}^{Ph}$ , respectively, in a concentration-based manner. Similarly, SBF is phosphorylated by Clb1/2 with rate  $k_{SbfClb}^{Ph}$ .

In order to exit the cell cycle, cells need to degrade cyclins using the APC/C. Our model accounts for two of its forms: APC/C<sup>Cdh1</sup> (CDH) and APC/C<sup>Cdc20</sup> (CDC), both of which can be present in an active (subscript a) and an inactive (subscript i) configuration.

$$\frac{d(CDH_i)}{dt} = r_{Cdh}^{Sy} - r_{Cdh}^{Ac} \cdot \frac{CDH_i/V_t}{j_{Cdh} + CDH_i/V_t} + r_{Cdh}^{In} \cdot \frac{CDH_a/V_t}{j_{Cdh} + CDH_a/V_t}, \quad (28)$$

$$\frac{d(CDH_a)}{dt} = r_{Cdh}^{Ac} \cdot \frac{CDH_i/V_t}{j_{Cdh} + CDH_i/V_t} - r_{Cdh}^{In} \cdot \frac{CDH_a/V_t}{j_{Cdh} + CDH_a/V_t}, \quad (29)$$

$$\frac{d(CDC_i)}{dt} = r_{Cdc}^{Sy} - r_{Cdc}^{Ac} \cdot \frac{CDC_i/V_t}{j_{Cdc} + CDC_i/V_t} + r_{Cdc}^{In} \cdot \frac{CDC_a/V_t}{j_{Cdc} + CDC_a/V_t}, \quad (30)$$

$$\frac{d(CDC_a)}{dt} = r_{Cdc}^{Ac} \cdot \frac{CDC_i/V_t}{j_{Cdc} + CDC_i/V_t} - r_{Cdc}^{In} \cdot \frac{CDC_a/V_t}{j_{Cdc} + CDC_a/V_t}, \quad (31)$$

where the Cdh1 and Cdc20 subunits are synthesised with rates  $r_{Cdh}^{Sy}$  and  $r_{Cdc}^{Sy}$  (see Eqs 32 and 33), respectively, and binding of these subunits to the APC/C is assumed to be instantaneous and limited by subunit availability. Based on previous models [43], activation and inactivation of the APC/C is assumed to occur via concentration-dependent, Michaelis-Menten-type kinetics with rates  $r^{Ac}$  and  $r^{In}$ , respectively. The corresponding Michaelis-Menten constants are denoted  $j_{Cdh}$  and  $j_{Cdc}$ . The rates of subunit synthesis and APC/C activation and inactivation were defined as follows:

$$r_{Cdh}^{Sy} = k_{V_o}^{Sy} \cdot GDTM \cdot \frac{GCN}{GD_t}, \quad (32)$$

$$r_{Cdc}^{Sy} = k_{V_o}^{Sy} \cdot GDTM \cdot \frac{GCN}{GD_t}, \quad (33)$$

$$r_{Cdh}^{Ac} = k_{Cdh}^{Ac} \cdot V_t + k_{CdhCdc}^{Ac} \cdot CDC_a, \quad (34)$$

$$r_{Cdh}^{In} = k_{CdhCln}^{In} \cdot CLN + k_{CdhClb}^{In} \cdot CLB, \quad (35)$$

$$r_{Cdc}^{Ac} = k_{CdcClb}^{Ac} \cdot CLB, \quad (36)$$

$$r_{Cdc}^{In} = k_{Cdc}^{In} \cdot V_t. \quad (37)$$

Here, synthesis of Cdh1 and Cdc20 occurs similar to SBF (described above) to a constant concentration of 1 AU/AV. APC/C<sup>Cdh1</sup> is activated with the constitutive rate  $k_{Cdh}^{Ac}$  and by active APC/C<sup>Cdc20</sup> with rate  $k_{CdhCdc}^{Ac}$ , while inactivation is mediated by Cln1/2 and Clb1/2 with rates  $k_{CdhCln}^{In}$  and  $k_{CdhClb}^{In}$ , respectively. Similarly, APC/C<sup>Cdc20</sup> is activated by Clb1/2 with rate  $k_{CdcClb}^{Ac}$  and inactivated with constitutive rate  $k_{Cdc}^{In}$ .

To account for genome replication and cell division, we introduced two events in our model. The first is triggered when Cln1/2 increase above a threshold concentration, which induces bud growth and genome duplication.

$$\begin{aligned} & \text{If } CLN/V_t \geq StartThr : \\ Gr_m = 0, Gr_d = 1, GD_t = 2 \cdot GD_t, GCN = 2 \cdot GCN, GW_t = 2 \cdot GW_t, GC_t = 2 \cdot GC_t. \end{aligned} \quad (38)$$

Similarly, cell division occurs when the combined concentration of Cln1/2 and Clb1/2 falls below the threshold that maintains mitosis.

$$\begin{aligned} & \text{If } (CLN + CLB)/V_t \leq MitosistThr : \\ Gr_m = 1, Gr_d = 0, GD_t = GD_t/2, GCN = GCN/2, GW_t = GW_t/2, GC_t = GC_t/2, \\ V_m = V_d, V_d = 0, TM = TM \cdot V_r, GITM = GITM \cdot V_r, GDTM = GDTM \cdot V_r, \\ CLN3 = CLN3 \cdot V_r, CLN = CLN \cdot V_r, CLB = CLB \cdot V_r, WHI = WHI \cdot V_r + WHI_n, \\ WHI_n = 0, WHI_p = WHI_p \cdot V_r, SBF = SBF \cdot V_r, SBF_p = SBF_p \cdot V_r, \\ WHISBF = WHISBF \cdot V_r, CDH_i = CDH_i \cdot V_r, CDH_a = CDH_a \cdot V_r, \\ CDC_i = CDC_i \cdot V_r, CDC_a = CDC_a \cdot V_r, \\ & \text{with } V_r = V_d/V_m. \end{aligned} \quad (39)$$

Note that we followed the daughter cell (bud) after budding as size control mainly takes place in these small, new-born cells [3–5]. Hence, at cell division, we assigned  $V_d$  to  $V_m$  (the daughter becomes the new ‘mother’ cell) and directed growth into the new cell. Moreover, the genome is split evenly, such that the new cell receives half of all gene-related variables. The remaining proteins are divided based on the volume ratio of mother and daughter cell before division ( $V_r$ ), assuming that these proteins can freely diffuse in the cytoplasm or nucleus. However, we assumed that all newly produced Whi5 is directed towards the daughter cell. This is consistent with experimental evidence showing a higher concentration of Whi5 in daughter cells compared to their mothers after division [13] and with the fact that mother cells exhibit a short G1 phase [4,5]. In particular, as mother cells do not increase significantly in volume after START, any newly produced Whi5 that remains in the mother cell would increase its Whi5 concentration above the previously passed threshold for START, thus extending the ‘old’ mother’s next G1-phase and leading to further mother-cell growth. Also note that we assumed transcriptionally active genes rapidly adapt to the new concentration of TM and hence multiplied these variables by  $V_r$  as well.

**Titration of nuclear sites model.** Our titration model is based on the principles of gene expression outlined above and largely employs the same equations than the inhibitor-dilution model. The main differences between the two models relate to the interactions of Cln3, Whi5 and SBF (see also [S1 Text](#)).

The growth in mother and daughter cell volume was modelled as described in Eqs 9 and 10, with both depending on transcriptionally active size-dependent genes. Similarly, Cln1/2 and Clb1/2 are synthesised from such genes following Eqs 12, 13 and 15–17. We modelled the interaction of Cln3, Whi5 and SBF according to the titration hypothesis put forward by Wang et al. [20]. In particular, we assumed that there is limited number of nuclear sites ( $NS_i$ ) for SBF binding. For the sake of simplicity, we only accounted for the SBF that is bound to these sites and neglected freely diffusing SBF, such that all SBF-related variables refer to SBF on nuclear

sites and total SBF ( $SBF_t$ ) is constant at

$$SBF_t = NS_t. \tag{40}$$

Cln3, Whi5 and SBF were assumed to interact in a two-step process (see S2B Fig). First, Whi5 binds to SBF and forms a Whi5:SBF complex ( $WHISBF$ ), which inhibits SBF activity. Subsequently, Cln3 can bind to form a trimeric Cln3:Whi5:SBF complex ( $CLN3WHISBF$ ) in which Whi5 becomes hypo-phosphorylated, causing the dissociation of Cln3 and leaving a hypo-phosphorylated, but still inhibited, Whi5-P:SBF complex ( $WHIpSBF$ ). This complex can either be dephosphorylated or hyper-phosphorylated by free Cln3, which liberates SBF and induces Cln1/2 expression. Forming a positive feedback, Cln1/2 promotes further hyper-phosphorylation of  $WHIpSBF$  and of free Whi5, preventing the re-inhibition of SBF. Following these considerations, the number of free Whi5 ( $WHI$ ) and phosphorylated Whi5 ( $WHI_p$ ) molecules is given by

$$\frac{d(WHI)}{dt} = -\frac{k_{WhiSbf}^{As}}{V_t} \cdot SBF \cdot WHI - r_{Whi}^{Ph} \cdot WHI + k_{Whi}^{Dp} \cdot WHI_p, \tag{41}$$

$$\frac{d(WHI_p)}{dt} = r_{Whi}^{Ph} \cdot WHI - k_{Whi}^{Dp} \cdot WHI_p + r_{Whip}^{Ph} \cdot WHIpSBF, \tag{42}$$

where  $k_{WhiSbf}^{As}$  denotes the rate constant for Whi5-SBF binding and  $k_{Whi}^{Dp}$  represents the dephosphorylation of Whi5. Free Whi5 is phosphorylated with rate  $r_{Whi}^{Ph}$  (see Eq 47), while hypo-phosphorylated Whi5 in Whi5:SBF complexes is hyper-phosphorylated with rate  $r_{Whip}^{Ph}$  (see Eq 48). Interaction of Cln3, Whi5 and SBF occurs according to

$$\frac{d(CLN3)}{dt} = r_{Cln3}^{Sy} - \frac{k_{Cln3Whi}^{As}}{V_t} \cdot CLN3 \cdot WHISBF + (k_{Cln3Whi}^{Ds} + k_{WhiCln3}^{Ph}) \cdot CLN3WHISBF - k_{Cln3}^{De} \cdot CLN3, \tag{43}$$

$$\frac{d(WHISBF)}{dt} = -\frac{k_{Cln3Whi}^{As}}{V_t} \cdot CLN3 \cdot WHISBF + (k_{Cln3Whi}^{Ds} + k_{Cln3}^{De}) \cdot CLN3WHISBF + k_{Whi}^{Dp} \cdot WHIpSBF + \frac{k_{WhiSbf}^{As}}{V_t} \cdot SBF \cdot WHI, \tag{44}$$

$$\begin{aligned} \frac{d(CLN3WHISBF)}{dt} &= \frac{k_{Cln3Whi}^{As}}{V_t} \cdot CLN3 \cdot WHISBF - (k_{Cln3Whi}^{Ds} + k_{WhiCln3}^{Ph} + k_{Cln3}^{De}) \cdot CLN3WHISBF, \end{aligned} \tag{45}$$

$$\frac{d(WHIpSBF)}{dt} = k_{WhiCln3}^{Ph} \cdot CLN3WHISBF - (r_{Whip}^{Ph} + k_{Whi}^{Dp}) \cdot WHIpSBF. \tag{46}$$

Here, Cln3 is synthesised and degraded with rate  $r_{Cln3}^{Sy}$  (see Eq 14) and  $k_{Cln3}^{De}$ , respectively, and it binds to and dissociates from Whi5:SBF complexes with rate  $k_{Cln3Whi}^{As}$  and  $k_{Cln3Whi}^{Ds}$ , respectively. Hypo-phosphorylation of Whi5 by Cln3 in the trimeric complexes occurs with rate constant  $k_{WhiCln3}^{Ph}$  and leads to Cln3 dissociation. This phosphorylation can be reversed with rate  $k_{Whi}^{Dp}$  or converted to hyper-phosphorylation with rate  $r_{Whip}^{Ph}$  (see Eq 48), which liberates SBF.

The phosphorylation rates of Whi5 were defined as follows

$$r_{\text{Whi}}^{\text{Ph}} = k_{\text{WhiCln}}^{\text{Ph}} \cdot \text{CLN}/V_t, \quad (47)$$

$$r_{\text{Whip}}^{\text{Ph}} = (k_{\text{WhipCln3}}^{\text{Ph}} \cdot \text{CLN3} + k_{\text{WhipCln}}^{\text{Ph}} \cdot \text{CLN})/V_t, \quad (48)$$

where the rate of free Whi5 phosphorylation by Cln1/2 is  $k_{\text{WhiCln}}^{\text{Ph}}$  and the rates of hyper-phosphorylation of *WHIpSBF* by Cln3 and Cln1/2 are  $k_{\text{WhipCln3}}^{\text{Ph}}$  and  $k_{\text{WhipCln}}^{\text{Ph}}$ , respectively. SBF on nuclear sites that is not inhibited by Whi5 (*SBF*) can be calculated from the conservation equation

$$\text{SBF} = \text{NS}_t - \text{WHISBF} - \text{CLN3WHISBF} - \text{WHIpSBF}.$$

As in the inhibitor-dilution model, SBF activity is additionally regulated by an inhibitory phosphorylation (Eqs 22 and 27), which is assumed to be independent of the other reaction steps SBF undergoes. Furthermore, the production of Whi5 and the dynamics of APC/ $C^{\text{Cdh1}}$  and APC/ $C^{\text{Cdc20}}$  were modelled as described before (Eqs 23, 24 and 28–37).

Similarly to Eqs 38 and 39, we introduced two events that represent *START* and cell division, respectively. An increase of the Cln1/2 concentration above a threshold initiates bud growth and genome replication, which, in the titration model, includes an increase in the number of nuclear sites and SBF complexes bound to them:

If  $\text{CLN}/V_t \geq \text{StartThr}$  :

$$\begin{aligned} Gr_m = 0, Gr_d = 1, GD_t = 2 \cdot GD_t, GCN = 2 \cdot GCN, GW_t = 2 \cdot GW_t, GC_t = 2 \cdot GC_t, \\ NS_t = 2 \cdot NS_t, SBF_p = 2 \cdot SBF_p \end{aligned} \quad (49)$$

At cell division, which is initiated when the combined concentration of Cln1/2 and Clb1/2 falls below the threshold that maintains mitosis, gene-related variables are divided equally between the two cells, while freely diffusing molecules are inherited based on the volume ratio of mother and daughter cell ( $V_r$ ).

If  $(\text{CLN} + \text{CLB})/V_t \leq \text{MitosistThr}$ :

$$\begin{aligned} Gr_m = 1, Gr_d = 0, GD_t = GD_t/2, GCN = GCN/2, GW_t = GW_t/2, GC_t = GC_t/2, \\ NS_t = NS_t/2, SBF_p = SBF_p/2, V_m = V_d, V_d = 0, TM = TM \cdot V_r, \\ GITM = GITM \cdot V_r, GDTM = GDTM \cdot V_r, CLN3 = CLN3 \cdot V_r, CLN = CLN \cdot V_r, \\ CLB = CLB \cdot V_r, WHI = WHI \cdot V_r + WHI_n, WHI_n = 0, WHI_p = WHI_p \cdot V_r, \\ WHISBF = WHISBF \cdot V_r, CLN3WHISBF = CLN3WHISBF \cdot V_r, \\ WHIpSBF = WHIpSBF \cdot V_r, CDH_i = CDH_i \cdot V_r, CDH_a = CDH_a \cdot V_r, CDC_i = CDC_i \cdot V_r, CDC_a = CDC_a \cdot V_r \end{aligned}$$

with  $V_r = V_d/V_m$ .

Again, the transcription machinery on genes is assumed to adjust rapidly to the new TM concentration, and so are the complexes of Whi5 and Cln3 with SBF on the nuclear sites.

## Computation

Both size-control models were prepared in the Systems Biology Toolbox 2 [44] for MatLab (version 9.1.0 R2016b) and simulated with the CVODE routine [45]. Bifurcation diagrams

were calculated using the freely available software XPP-Aut [46]. Models are provided as S1–S3 Files in the Supplement and different versions are available at [www.cellcycle.org.uk/publication](http://www.cellcycle.org.uk/publication). Model files were also deposited in BioModels [47] and assigned the identifiers MODEL1803220001 and MODEL1803220002. Parameter values and initial conditions are listed in S1–S4 Tables and S5 Table shows the changes required to simulate ploidy mutants in Figs 3, 4, S3 and S4.

In order to simulate cells of different sizes (e.g. in Fig 2F and 2G), we varied the specific growth rate, with higher growth rates producing larger cells. In particular, the specific growth rate ( $\mu$ ) in our model follows from Eqs 9 and 10 as

$$\mu = \frac{1}{V_t} \frac{d(V_t)}{dt} = k_{V_o}^{Sy} \cdot \frac{GDTM}{V_t} \cdot \frac{GCN}{GD_t}$$

Since  $GD_t \gg GI_t$  and almost all of the TM is bound to genes for the cell sizes we study here, the amount of transcriptionally active size-dependent genes can be approximated by the total number of TM ( $GDTM \approx TM_t$ ). Moreover, we can calculate the transcriptional capacity per unit cell volume as

$$\frac{TM_t}{V_t} = \frac{k_{Tm}^{Sy}}{k_{V_o}^{Sy}}$$

Taken together this gives

$$\mu \approx k_{V_o}^{Sy} \cdot \frac{k_{Tm}^{Sy}}{k_{V_o}^{Sy}} \cdot \frac{GCN}{GD_t}$$

demonstrating that by changing both  $k_{V_o}^{Sy}$  and  $k_{Tm}^{Sy}$  by the same factor, we can change the specific growth rate, while still maintaining the same transcriptional capacity per unit cell volume and thus similar protein expression. Accordingly, for simulations in Fig 2F and 2G,  $k_{V_o}^{Sy}$  and  $k_{Tm}^{Sy}$  were multiplied by a factor  $f \in [0.75, 1.25]$ . For simulations in Figs 5 and S5, we followed a single cell lineage over a large number of divisions to correlate cell sizes at different cell cycle stages. To obtain different cell sizes, we again varied the growth rate as described above, assuming that it changes at cell division. In particular, we assumed that the specific growth rate in the next cycle ( $\mu_{n+1}$ ) is partly inherited from the mother cell's growth rate ( $\mu_n$ ) and partly influenced by stochasticity, e.g., by the random distribution of molecules at cell division, using

$$\mu_{n+1} = 0.5 \cdot \mu_n + 0.5 \cdot \bar{\mu} \cdot (1 + \mathcal{N}(0, 0.04)),$$

where  $\bar{\mu}$  is the average growth rate and  $\mathcal{N}(0, \sigma)$  a normally distributed random variable with mean 0 and variance  $\sigma$ .

## Supporting information

**S1 File. Model of size-dependent and size-independent protein expression.**  
(TXT)

**S2 File. Inhibitor-dilution model for budding yeast size control.**  
(TXT)

**S3 File. Titration-of-nuclear-sites model for budding yeast size control.**  
(TXT)

**S1 Fig. Related to Fig 1.** Expression patterns of genes with different equilibrium constants for TM binding, ranging from high (size-independent) to low (size-dependent) affinity. (A) Gene

occupation by TM in dependence on cell volume. (B) Relative protein concentration (normalised to initial concentration) in dependence on time in a growing cell. (C) Protein synthesis rates in haploid (solid) and diploid (dashed) cells. Curves in left panel overlap.

(TIF)

**S2 Fig. Related to Figs 2 and 4.** (A) Scheme of SBF inhibition in the inhibitor-dilution model. Whi5 strongly binds to SBF in a concentration-based manner, causing SBF inhibition. Both free and complexed Whi5 can be phosphorylated by Cln3, Cln1/2 and Clb1/2. Phosphorylation of SBF:Whi5 complexes leads to their dissociation, which activates SBF. (B) Scheme of SBF inhibition in the titration model. Whi5 strongly binds to SBF, which occupies a fixed number of nuclear sites. Cln3 strongly binds to Whi5:SBF, slowly hypo-phosphorylating the complex and dissociating in the process. Hypo-phosphorylated Whi5:SBF can return to the unphosphorylated state. However, when free Cln3 or Cln1/2 are available, Whi5 becomes hyper-phosphorylated leading to Whi5 dissociation and SBF activation. Subsequently, the free pool of Whi5 is phosphorylated by Cln1/2. Note that in both models, active SBF drives the synthesis of Cln1/2, which accelerates Whi5 phosphorylation and SBF activation (see Fig 2A).

This positive feedback establishes an abrupt toggle switch at START.

(TIF)

**S3 Fig. Related to Fig 3.** (A) Amount of Whi5 and Cln3 (upper panels) and cell volume (lower panels) in haploid cells with one *WHI5* copy (left), diploid cells with one *WHI5* copy (middle) and diploid cells with two *WHI5* copies (right). Note the increase in Whi5 synthesis (increased slope during synthesis period) and cell volume in the latter case. (B, C) Same as in Fig 3B and 3C except that the S/G2/M duration of all diploid cells was increased by approximately 10% based on experiments in Ref. [13].

(TIF)

**S4 Fig. Related to Fig 4.** (A) Amount of Whi5:SBF, Whi5:SBF:Cln3 and active SBF (upper panels), and cell volume (lower panels) in haploid (left) and diploid (right) cells with one *WHI5* copy in the titration model. Note the increase in cell volume for diploid cells due to the presence of twice the number of SBF complexes on binding sites (sum of the three species shown). (B, C) Same as in Fig 4E and 4F except that Cln3 synthesis in diploid cells with one *CLN3* was manually increased by a factor of 0.7. (D) Simulated cell size at START for a normal haploid cell (wild-type) and a haploid cell harbouring a plasmid that contains SBF binding sites (+ nuclear sites) following the experiment in Fig 7 of Ref. [20]. The total number of binding sites was increased by ~30%.

(TIF)

**S5 Fig. Related to Fig 5.** (A) Duration of the indicated cell cycle phase or the whole cycle with respect to volume at the beginning of the phase for the simulations in Fig 5. Note the logarithmic scaling of the x-axis. (B) Same as in Fig 5B, except that the amount of Whi5 at cell birth was manually set to a constant, birth-size-independent value. This results in an almost ideal G1 sizer (slope of -0.95 for volume added in G1 versus birth size). Note that the phenomenological adder over the whole cell cycle disappears in this case (slope of -0.49 for volume added over the whole cell cycle versus birth size).

(TIF)

**S6 Fig.** (A) Schematic of the SBF-increase model. In early G1, Whi5 outnumbers SBF and prevents its activation. A fraction of Whi5 is phosphorylated by Cln3 and does not participate in inhibition. As cells grow, the SBF concentration increases such that SBF is able to overcome inhibition and induce Cln1 and Cln2 synthesis. Whi5 phosphorylation then liberates the rest of

the SBF pool. **(B)** Concentration of Whi5 and Cln3 as well as total and active SBF in a growing cell. Vertical dashed line marks  $START$ . **(C)** Stable (solid) and unstable (dashed) steady states of active SBF with respect to cell volume in the SBF-increase model. Arrow indicates  $START$  transition. **(D)** Concentration of cell cycle regulators (top) and cell volume (bottom) over multiple generations. Dashed and dotted lines mark  $START$  and division, respectively. **(E)** Simulation of Whi5 and Cln3 synthesis rates in haploid and diploid cells with the indicated copy number of *WHI5* and *CLN3*. **(F)** Mean cell volume in G1 for data in [13] (light bars) and simulations in E (dark bars). Values were normalized to haploid cells with one *WHI5* copy for each case. (TIF)

**S1 Text. Differences between inhibitor-dilution and titration model.**

(DOCX)

**S2 Text. Model for increasing SBF concentration.**

(DOCX)

**S1 Table. Parameters used in both size-control models.**

(DOCX)

**S2 Table. Parameters specific to the inhibitor-dilution model.**

(DOCX)

**S3 Table. Parameters specific to the titration-of-nuclear-sites model.**

(DOCX)

**S4 Table. Non-zero initial conditions for both models.**

(DOCX)

**S5 Table. Parameters changes for ploidy mutants.**

(DOCX)

## Author Contributions

**Conceptualization:** Frank S. Heldt, John J. Tyson, Béla Novák.

**Formal analysis:** Frank S. Heldt, Reece Lunstone, Béla Novák.

**Funding acquisition:** John J. Tyson, Béla Novák.

**Investigation:** Frank S. Heldt, Reece Lunstone, John J. Tyson, Béla Novák.

**Methodology:** Frank S. Heldt, John J. Tyson, Béla Novák.

**Software:** Frank S. Heldt, Reece Lunstone.

**Supervision:** Béla Novák.

**Validation:** Frank S. Heldt.

**Visualization:** Frank S. Heldt.

**Writing – original draft:** Frank S. Heldt, Béla Novák.

**Writing – review & editing:** Frank S. Heldt, John J. Tyson, Béla Novák.

## References

1. Ginzberg MB, Kafri R, Kirschner M. Cell biology. On being the right (cell) size. *Science*. 2015; 348: 1245075. <https://doi.org/10.1126/science.1245075> PMID: 25977557



2. Amodeo AA, Skotheim JM. Cell-Size Control. *Cold Spring Harb Perspect Biol.* 2016; 8: a019083. <https://doi.org/10.1101/cshperspect.a019083> PMID: 26254313
3. Johnston GC, Pringle JR, Hartwell LH. Coordination of growth with cell division in the yeast *Saccharomyces cerevisiae*. *Exp Cell Res.* 1977; 105: 79–98. [https://doi.org/10.1016/0014-4827\(77\)90154-9](https://doi.org/10.1016/0014-4827(77)90154-9) PMID: 320023
4. Hartwell LH, Unger MW. Unequal division in *Saccharomyces cerevisiae* and its implications for the control of cell division. *J Cell Biol.* 1977; 75: 422–435. <https://doi.org/10.1083/jcb.75.2.422> PMID: 400873
5. Talia SD, Skotheim JM, Bean JM, Siggia ED, Cross FR. The effects of molecular noise and size control on variability in the budding yeast cell cycle. *Nature.* 2007; 448: 947–951. <https://doi.org/10.1038/nature06072> PMID: 17713537
6. Nurse P. Genetic control of cell size at cell division in yeast. *Nature.* 1975; 256: 547–551. <https://doi.org/10.1038/256547a0> PMID: 1165770
7. Fantes P, Nurse P. Control of cell size at division in fission yeast by a growth-modulated size control over nuclear division. *Exp Cell Res.* 1977; 107: 377–386. [https://doi.org/10.1016/0014-4827\(77\)90359-7](https://doi.org/10.1016/0014-4827(77)90359-7) PMID: 872891
8. Keifenheim D, Sun X-M, D'Souza E, Ohira MJ, Magner M, Mayhew MB, et al. Size-Dependent Expression of the Mitotic Activator Cdc25 Suggests a Mechanism of Size Control in Fission Yeast. *Curr Biol.* 2017; 27: 1491–1497.e4. <https://doi.org/10.1016/j.cub.2017.04.016> PMID: 28479325
9. Sudbery PE, Grant WD. The control of mitosis in *Physarum polycephalum*: The effect of lowering the DNA: Mass ratio by UV irradiation. *Exp Cell Res.* 1975; 95: 405–415. [https://doi.org/10.1016/0014-4827\(75\)90566-2](https://doi.org/10.1016/0014-4827(75)90566-2) PMID: 1238278
10. Sudbery PE, Grant WD. The control of mitosis in *Physarum polycephalum*: the effect of delaying mitosis and evidence for the operation of the control mechanism in the absence of growth. *J Cell Sci.* 1976; 22: 59–65. PMID: 135767
11. Tyson J, Garcia-Herdugo G, Sachsenmaier W. Control of nuclear division in *Physarum polycephalum*: Comparison of cycloheximide pulse treatment, UV irradiation, and heat shock. *Exp Cell Res.* 1979; 119: 87–98. [https://doi.org/10.1016/0014-4827\(79\)90338-0](https://doi.org/10.1016/0014-4827(79)90338-0) PMID: 761604
12. Schmoller KM, Skotheim JM. The Biosynthetic Basis of Cell Size Control. *Trends Cell Biol.* 2015; 25: 793–802. <https://doi.org/10.1016/j.tcb.2015.10.006> PMID: 26573465
13. Schmoller KM, Turner JJ, Kõivomägi M, Skotheim JM. Dilution of the cell cycle inhibitor Whi5 controls budding-yeast cell size. *Nature.* 2015; 526: 268–272. <https://doi.org/10.1038/nature14908> PMID: 26390151
14. Koch C, Nasmyth K. Cell cycle regulated transcription in yeast. *Curr Opin Cell Biol.* 1994; 6: 451–459. [https://doi.org/10.1016/0955-0674\(94\)90039-6](https://doi.org/10.1016/0955-0674(94)90039-6) PMID: 7917338
15. Costanzo M, Nishikawa JL, Tang X, Millman JS, Schub O, Breikreuz K, et al. CDK Activity Antagonizes Whi5, an Inhibitor of G1/S Transcription in Yeast. *Cell.* 2004; 117: 899–913. <https://doi.org/10.1016/j.cell.2004.05.024> PMID: 15210111
16. de Bruin RAM, McDonald WH, Kalashnikova TI, Yates J III, Wittenberg C. Cln3 Activates G1-Specific Transcription via Phosphorylation of the SBF Bound Repressor Whi5. *Cell.* 2004; 117: 887–898. <https://doi.org/10.1016/j.cell.2004.05.025> PMID: 15210110
17. Tyers M, Tokiwa G, Futcher B. Comparison of the *Saccharomyces cerevisiae* G1 cyclins: Cln3 may be an upstream activator of Cln1, Cln2 and other cyclins. *EMBO J.* 1993; 12: 1955–1968. PMID: 8387915
18. Sachsenmaier W, Remy U, Plattner-Schobel R. Initiation of synchronous mitosis in *Physarum polycephalum*: A model of the control of cell division in eukariots. *Exp Cell Res.* 1972; 73: 41–48. [https://doi.org/10.1016/0014-4827\(72\)90099-7](https://doi.org/10.1016/0014-4827(72)90099-7) PMID: 4260954
19. Fantes PA, Grant WD, Pritchard RH, Sudbery PE, Wheals AE. The regulation of cell size and the control of mitosis. *J Theor Biol.* 1975; 50: 213–244. [https://doi.org/10.1016/0022-5193\(75\)90034-X](https://doi.org/10.1016/0022-5193(75)90034-X) PMID: 1127959
20. Wang H, Carey LB, Cai Y, Wijnen H, Futcher B. Recruitment of Cln3 Cyclin to Promoters Controls Cell Cycle Entry via Histone Deacetylase and Other Targets. *PLOS Biol.* 2009; 7: e1000189. <https://doi.org/10.1371/journal.pbio.1000189> PMID: 19823669
21. Chandler-Brown D, Schmoller KM, Winetraub Y, Skotheim JM. The Adder Phenomenon Emerges from Independent Control of Pre- and Post-Start Phases of the Budding Yeast Cell Cycle. *Curr Biol.* 2017; 27: 2774–2783.e3. <https://doi.org/10.1016/j.cub.2017.08.015> PMID: 28889980
22. Zhurinsky J, Leonhard K, Watt S, Marguerat S, Bähler J, Nurse P. A Coordinated Global Control over Cellular Transcription. *Curr Biol.* 2010; 20: 2010–2015. <https://doi.org/10.1016/j.cub.2010.10.002> PMID: 20970341
23. Coulon A, Chow CC, Singer RH, Larson DR. Eukaryotic transcriptional dynamics: from single molecules to cell populations. *Nat Rev Genet.* 2013; 14: 572–584. <https://doi.org/10.1038/nrg3484> PMID: 23835438

24. Voss TC, Hager GL. Dynamic regulation of transcriptional states by chromatin and transcription factors. *Nat Rev Genet.* 2014; 15: 69–81. <https://doi.org/10.1038/nrg3623> PMID: 24342920
25. Skotheim JM, Di Talia S, Siggia ED, Cross FR. Positive feedback of G1 cyclins ensures coherent cell cycle entry. *Nature.* 2008; 454: 291–296. <https://doi.org/10.1038/nature07118> PMID: 18633409
26. Charvin G, Oikonomou C, Siggia ED, Cross FR. Origin of irreversibility of cell cycle start in budding yeast. *PLoS Biol.* 2010; 8: e1000284. <https://doi.org/10.1371/journal.pbio.1000284> PMID: 20087409
27. Turner JJ, Ewald JC, Skotheim JM. Cell Size Control in Yeast. *Curr Biol.* 2012; 22: R350–R359. <https://doi.org/10.1016/j.cub.2012.02.041> PMID: 22575477
28. Willis L, Huang KC. Sizing up the bacterial cell cycle. *Nat Rev Microbiol.* 2017; 15: 606–620. <https://doi.org/10.1038/nrmicro.2017.79> PMID: 28804128
29. Williamson DH, Scopes AW. The distribution of nucleic acids and protein between different sized yeast cells. *Exp Cell Res.* 1961; 24: 151–153. [https://doi.org/10.1016/0014-4827\(61\)90258-0](https://doi.org/10.1016/0014-4827(61)90258-0) PMID: 13785539
30. Crissman HA, Steinkamp JA. Rapid, simultaneous measurement of DNA, protein, and cell volume in single cells from large mammalian cell populations. *J Cell Biol.* 1973; 59: 766–771. PMID: 4128323
31. Schmidt EE, Schibler U. Cell size regulation, a mechanism that controls cellular RNA accumulation: consequences on regulation of the ubiquitous transcription factors Oct1 and NF-Y and the liver-enriched transcription factor DBP. *J Cell Biol.* 1995; 128: 467–483. <https://doi.org/10.1083/jcb.128.4.467> PMID: 7532171
32. Padovan-Merhar O, Nair GP, Biaesch AG, Mayer A, Scarfone S, Foley SW, et al. Single mammalian cells compensate for differences in cellular volume and DNA copy number through independent global transcriptional mechanisms. *Mol Cell.* 2015; 58: 339–352. <https://doi.org/10.1016/j.molcel.2015.03.005> PMID: 25866248
33. Kempe H, Schwabe A, Crémazy F, Verschure PJ, Bruggeman FJ. The volumes and transcript counts of single cells reveal concentration homeostasis and capture biological noise. *Mol Biol Cell.* 2015; 26: 797–804. <https://doi.org/10.1091/mbc.E14-08-1296> PMID: 25518937
34. Soifer I, Robert L, Amir A. Single-Cell Analysis of Growth in Budding Yeast and Bacteria Reveals a Common Size Regulation Strategy. *Curr Biol.* 2016; 26: 356–361. <https://doi.org/10.1016/j.cub.2015.11.067> PMID: 26776734
35. Dorsey S, Tollis S, Cheng J, Black L, Notley S, Tyers M, et al. G1/S Transcription Factor Copy Number Is a Growth-Dependent Determinant of Cell Cycle Commitment in Yeast. *Cell Syst.* 2018; 6: 539–554. e11. <https://doi.org/10.1016/j.cels.2018.04.012> PMID: 29792825
36. Campos M, Surovtsev IV, Kato S, Paintdakhi A, Beltran B, Ebmeier SE, et al. A Constant Size Extension Drives Bacterial Cell Size Homeostasis. *Cell.* 2014; 159: 1433–1446. <https://doi.org/10.1016/j.cell.2014.11.022> PMID: 25480302
37. Taheri-Araghi S, Bradde S, Sauls JT, Hill NS, Levin PA, Paulsson J, et al. Cell-Size Control and Homeostasis in Bacteria. *Curr Biol.* 2015; 25: 385–391. <https://doi.org/10.1016/j.cub.2014.12.009> PMID: 25544609
38. Tyers M, Tokiwa G, Nash R, Futcher B. The Cln3-Cdc28 kinase complex of *S. cerevisiae* is regulated by proteolysis and phosphorylation. *EMBO J.* 1992; 11: 1773–1784. PMID: 1316273
39. Gillespie DT. Stochastic Simulation of Chemical Kinetics. *Annu Rev Phys Chem.* 2007; 58: 35–55. <https://doi.org/10.1146/annurev.physchem.58.032806.104637> PMID: 17037977
40. Nasmyth K, Dirick L. The role of SWI4 and SWI6 in the activity of G1 cyclins in yeast. *Cell.* 1991; 66: 995–1013. [https://doi.org/10.1016/0092-8674\(91\)90444-4](https://doi.org/10.1016/0092-8674(91)90444-4) PMID: 1832338
41. Amon A, Tyers M, Futcher B, Nasmyth K. Mechanisms that help the yeast cell cycle clock tick: G2 cyclins transcriptionally activate G2 cyclins and repress G1 cyclins. *Cell.* 1993; 74: 993–1007. [https://doi.org/10.1016/0092-8674\(93\)90722-3](https://doi.org/10.1016/0092-8674(93)90722-3) PMID: 8402888
42. Schwab M, Lutum AS, Seufert W. Yeast Hct1 Is a Regulator of Clb2 Cyclin Proteolysis. *Cell.* 1997; 90: 683–693. [https://doi.org/10.1016/S0092-8674\(00\)80529-2](https://doi.org/10.1016/S0092-8674(00)80529-2) PMID: 9288748
43. Tyson JJ, Novak B. Regulation of the eukaryotic cell cycle: molecular antagonism, hysteresis, and irreversible transitions. *J Theor Biol.* 2001; 210: 249–263. <https://doi.org/10.1006/jtbi.2001.2293> PMID: 11371178
44. Schmidt H, Jirstrand M. Systems Biology Toolbox for MATLAB: a computational platform for research in systems biology. *Bioinformatics.* 2006; 22: 514–515. <https://doi.org/10.1093/bioinformatics/bti799> PMID: 16317076
45. Cohen S, Hindmarsh AC. CVODE, a stiff/nonstiff ODE solver in C. *Computers in Physics.* 1996. pp. 138–143.
46. Ermentrout B. Simulating, Analyzing, and Animating Dynamical Systems [Internet]. Society for Industrial and Applied Mathematics; 2002. <https://doi.org/10.1137/1.9780898718195>
47. Chelliah V, Juty N, Ajmera I, Ali R, Dumousseau M, Glont M, et al. BioModels: ten-year anniversary. *Nucleic Acids Res.* 2015; 43: D542–D548. <https://doi.org/10.1093/nar/gku1181> PMID: 25414348